

Multi-isotopic composition ($\delta^7\text{Li}$ - $\delta^{11}\text{B}$ - δD - $\delta^{18}\text{O}$) of rainwaters in France: origin and spatio-temporal characterization

Romain Millot^{1*}, Emmanuelle Petelet-Giraud², Catherine Guerrot¹ and Philippe Négrel¹

1: BRGM, Metrology Monitoring Analysis Department, Orléans, France

2: BRGM, Water Department, Orléans, France

* Corresponding author, e-mail: r.millot@brgm.fr, Fax: + 33 2 38 64 37 11

Abstract

Lithium (Li) and boron (B) concentrations and isotope measurements for 45 monthly rainwater samples collected over a 1-year period from four different sites in France, from coastal and inland locations (Brest, Dax, Orléans and Clermont-Ferrand) are reported. This is the first study of Li and B isotope ratios in rainwater samples collected over a long time period at a national scale. The range of Li and B isotopic variations in these rainwaters are measured to enable the determination of the origin of these elements in rainwaters and the characterization of both the seasonal and spatio-temporal effects for $\delta^7\text{Li}$ and $\delta^{11}\text{B}$ signatures in rainwaters. Lithium and boron concentrations are low in rainwater samples, ranging from 0.004 to 0.292 $\mu\text{mol/L}$ and from 0.029 to 6.184 $\mu\text{mol/L}$, respectively. $\delta^7\text{Li}$ and $\delta^{11}\text{B}$ values in rainwaters also show a great range of variation between +3.2 and +95.6‰ and between -3.3 and +40.6‰ over a period of one year, respectively, for $\delta^7\text{Li}$ and $\delta^{11}\text{B}$, clearly different from the signature of seawater. Seasonal effects (i.e. rainfall amount and month) is not the main factor controlling element concentrations and isotopic variations. $\delta^7\text{Li}$ and $\delta^{11}\text{B}$ values in rainwaters are clearly different from one site to another, indicating the variable contribution of sea salts in the rainwater depending on the sampling site (coastal vs. inland: also called the distance-from-the-coast-effect). This is well illustrated when wind direction data (origin of air masses) is included. We found that seawater is not the main supplier of dissolved atmospheric lithium and boron, and non-sea-salt sources (i.e. crustal, anthropogenic, biogenic) should also be taken into account when Li and B isotopes are considered in hydrogeochemistry as an input to surface waters and groundwater bodies as a recharge. The isotopic variations of the water molecule, vector of the dissolved B and Li, are also investigated and reported as a contour map for $\delta^{18}\text{O}$ values based on compiled data including more than 400 $\delta^{18}\text{O}$ values from throughout France. This $\delta^{18}\text{O}$ map could be used as a reference for future studies dealing with $\delta^{18}\text{O}$ recharge signature in relation the characterization of surface waters and/or groundwater bodies.

Keywords: lithium isotopes, boron isotopes, hydrogen isotopes, oxygen isotopes, rainwaters, France

8 365 words (without references and captions)

40 1. INTRODUCTION

41
42 Atmospheric aerosols including sea salts, crustal dusts, biogenic materials and
43 anthropogenic emissions are the main sources of chemical elements in rainwaters (Junge
44 1963). The determination of the chemical composition of rainwater provides an
45 understanding of the source types that contribute to rainwater chemistry and enhances our
46 understanding of the dispersion of elements, whether pollutants or not, and their potential
47 impact on hydrosystems through precipitation and wet deposition processes (Berner and
48 Berner 1987).

49 The aim of this study is to present the results of the first study of both Li and B isotope ratios
50 in rainwater samples collected over a long time period (i.e. monthly rainfall events over one
51 year, Négrel et al. 2007) at a national scale. In addition, the stable isotopes of the water
52 molecule (δD and $\delta^{18}O$) are also reported here for the same locations (Brest, Dax and
53 Orléans) so that we can discuss the Li and B isotope data in the same context and to provide
54 a framework for the main processes affecting the isotope signatures of the rainwater. Since
55 rainwater is the main input in hydrogeological systems, monitoring the H-O-Li-B isotopic
56 compositions of rainwater at the national scale should enable us to compile a reference
57 system of meteoric isotopic signatures for all of France, as an addition to the Sr isotopes
58 data previously reported by Négrel et al. (2007).

59 The recent development of new isotopic techniques (e.g. lithium and boron: δ^7Li , $\delta^{11}B$) to
60 investigate aquifer systems has highlighted the gap in knowledge of the atmospheric inputs
61 that are the major contributor to groundwater recharge (Widory et al. 2005, Millot et al. 2007).
62 In this context, a knowledge of the spatial and temporal variability of the isotopic
63 compositions of rainwater appears to be essential for hydrogeological investigations and also
64 for sustainable water management.

65 This paper presents, firstly, the hydrogen and oxygen isotope data from the French Isotopic
66 Data Base (BDISO, 2007), in the form of a contour map linked to data from neighboring
67 countries and, secondly, boron and lithium isotopic data on selected samples from this
68 French monitoring network, part of the international database of the Global Network of
69 Isotopes in Precipitation (GNIP, 2007) managed by the International Agency of the Atomic
70 Energy (IAEA).

71 The characterization of δ^7Li and $\delta^{11}B$ signatures in rainwaters is of major importance if we
72 wish to increase our knowledge of the external cycles of these elements and, more
73 specifically in the field of hydrogeochemistry, characterize the Li and B isotope signatures of
74 the rainwater input to surface waters and/or groundwater bodies as a recharge.

75 To date, one measurement of δ^7Li (+14.3‰ \pm 0.7) has been reported in the literature for a
76 rainwater event collected in Hawaii (Pistiner and Henderson 2003) and another (+33.3‰),

77 slightly higher than the seawater signature, for a snow sample collected in Iceland (Pogge
78 von Strandmann et al. 2006).

79 On the other hand, $\delta^{11}\text{B}$ signatures of rainwaters are more circumscribed (Miyata et al. 2000,
80 Chetelat et al. 2005, Rose-Koga et al. 2006, Chetelat et al. 2009). Indeed, previous work on
81 the characterization of $\delta^{11}\text{B}$ signatures in rainwaters have shown that seawater may be a
82 major supplier of atmospheric boron, and that boron isotopic fractionation during evaporation
83 from seawater and removal from the atmosphere may account for the large variations of $\delta^{11}\text{B}$
84 signatures observed in the atmosphere and in rainwater (Miyata et al. 2000). In addition, it
85 has been also shown that boron isotopes in rainwater are potentially good tracers of biomass
86 burning (Chetelat et al. 2005) and anthropogenic contamination of the atmosphere in a
87 polluted environment (Chetelat et al. 2009).

88 The present study aims, therefore, at investigating Li and B isotope signatures in the rainfall
89 input, which should be identified in either surface water or groundwater since the sources of
90 Li and B both are atmospheric, the dissolution of Li- and B-bearing minerals, biogenic and/or
91 anthropogenic. This study also aims to more accurately define the input of Li and B to either
92 surface water or groundwater and place constraints on the $\delta^7\text{Li}$ and $\delta^{11}\text{B}$ values, which
93 should be corrected for atmospheric input, in order to characterize the anthropogenic
94 signature and/or the signature derived from water-rock interactions.

95

96

2. RAINWATER SAMPLES

97

2.1. Sampling sites

98

99
100 Monthly rain water samples were collected at five different locations throughout France
101 (Brest, Dax, Orléans, Thonon and Avignon, Fig. 1). They constitute the French monitoring
102 network, which is part of the IAEA/IOW Global Network for Isotopes in Précipitation (GNIP
103 2007) for isotopes of the water molecule. The long-term monthly monitoring consists in
104 sampling rainwater in Avignon (from May-97 to Dec-02, n=60), Brest (from Apr-96 to May-03,
105 n=83), Dax (from Oct-97 to Apr-04, n=74), Orléans (from Mar-96 to May-04, n=96) and
106 Thonon (from Mar-95 to Dec-02, n=89).

107 Three of these sampling sites were monitored between 2003 and 2004 for B and Li isotopes.
108 One, Brest, is located in the northwest of France (N 48.24, W 04.31), less than 5 km from the
109 Atlantic Ocean. Another, Dax, is located in the southwest of France (N 43.44, W 01.03), 30
110 km from the Atlantic Ocean. The third, Orléans (N 47.54, E 01.52), is located 400 km from
111 the Atlantic Ocean. A fourth B and Li isotope sampling site is located near Clermont-Ferrand
112 (N 45.46, E 03.04), in the Massif Central, 200 km upstream from Orléans. Rainwater

113 samples were monitored here between 1994 and 1995. The Mediterranean Sea is 300 km to
114 the south and the Atlantic Ocean is 380 km to the west.

115

116 **2.2. Sampling technique**

117

118 A direct polycarbonate funnel (Négrel et al. 1997), 12 cm in diameter and with an area of ~
119 110 cm², was used to collect the rainfall samples in Brest, Dax and Orléans. This apparatus
120 enables precipitation measurement by direct reading, without the need for preliminary
121 transfer into a measurement test tube. The rainwater was stored in a polypropylene jerrycan
122 to avoid any evaporation or modification of the sample. The accumulation of daily samples
123 enabled a monthly sample of rain to be obtained.

124 An automatic precipitation sampler was also designed for collecting rainwater samples at the
125 site near Clermont-Ferrand (Négrel and Roy 1998). The basic requirements for our collector
126 were automatic detection and collection of rainfall, elimination of dry fallout, collection of
127 frozen precipitation and prevention of sample contamination. A removable PVC lid covers the
128 funnel when no rain is falling. The cover opens to expose the funnel when electrical contact
129 is made in the rain detector. A polypropylene funnel (45 cm in diameter) was used to collect
130 the rainfall.

131 After monthly sample collection, 100 mL were used for δD and $\delta^{18}O$ determination. The rest
132 of the rainwater samples were filtered through pre-cleaned 0.45 μm acetate filters using a
133 pre-cleaned Nalgene filter apparatus and the filtrate was separated into two aliquots. From
134 this: (i) 100 and 1000 mL were acidified with double-distilled nitric acid (pH = 2) and stored in
135 pre-cleaned polyethylene bottles for major-cation analysis and lithium isotope ratio and
136 elemental Li and B determinations, and (ii) 500 mL were stored unacidified in polyethylene
137 bottles for anion analysis and B isotope ratio measurements.

138

139

139 **3. ANALYTICAL METHODS**

140

141 **3.1. Chemical parameters and stable isotopes of the water molecule**

142

143 The rainwater samples were chemically analysed by atomic absorption spectrometry (Ca,
144 Na, K, and Mg concentrations, accuracy 5%), ion chromatography (Cl, SO₄ and NO₃
145 concentrations, accuracy 5%) and inductively coupled plasma mass spectrometry (Li and B
146 concentrations, accuracy 5%). Accuracy and precision for major and trace elements was
147 verified by repeated measurements of standard materials during the course of this study:
148 namely Ion96-3 and LGC6020 for cations and anions and pure Li and B standard solutions
149 (Merck) for Li and B determinations.

150 Oxygen and deuterium measurements were performed by various French laboratories using
151 a standardised method. At BRGM's laboratory, a Finnigan MAT 252 mass spectrometer was
152 used with a precision of 0.1‰ for $\delta^{18}\text{O}$ and 0.8‰ for δD (vs. SMOW). Isotopic compositions
153 are reported in the usual δ -scale (in ‰) according to $\delta_{\text{sample}} (\text{‰}) = \{(R_{\text{sample}}/R_{\text{standard}}) - 1\} \times 10^3$,
154 where R is either the $^2\text{H}/^1\text{H}$ or the $^{18}\text{O}/^{16}\text{O}$ atomic ratio.

155 In the present work, it was challenging to measure Li and B isotope compositions in
156 rainwater samples due to their low content (a few $\mu\text{mol/L}$). We, therefore, developed new
157 sensitive techniques (Millot et al. 2004a, 2004b, Guerrot et al. 2010) in order to be able to
158 accurately and precisely determine $\delta^7\text{Li}$ and $\delta^{11}\text{B}$ for rainwater samples.

159

160 **3.2. Lithium isotopes**

161

162 Lithium isotopic compositions were measured using a Neptune Multi Collector ICP-MS
163 (Thermo Fischer Scientific). $^7\text{Li}/^6\text{Li}$ ratios were normalized to the L-SVEC standard solution
164 (NIST SRM 8545, Flesch et al. 1973) following the standard-sample bracketing method (see
165 Millot et al. 2004a for more details). The analytical protocol involves the acquisition of 15
166 ratios with 16 s integration time per ratio, and yields in-run precision better than 0.2‰ ($2\sigma_m$, 2
167 x Standard Error). Blank values are low, (i.e. 0.2‰), and 5 minutes wash time is enough to
168 reach a stable background value.

169 The samples must be prepared beforehand with chemical separation/purification by ion
170 chromatography in order to produce a pure mono-elemental solution. Chemical separation of
171 Li from the matrix was done prior to the mass analysis, following a procedure modified from
172 the technique of James and Palmer (2000), using a cationic resin (a single column filled with
173 3 mL of BioRad AG[®] 50W-X12 resin, 200-400 mesh) and HCl acid media (0.2N) for 30 ng of
174 Li. Blanks for the total chemical extraction were less than 30 pg of Li, which is negligible
175 since it represents a 10^{-3} blank/sample ratio.

176 Successful quantitative measurement of Li isotopic compositions requires 100% Li recovery
177 during laboratory processing. Therefore, frequent column calibration was done and repeated
178 analyses of L-SVEC standard processed through columns shows 100% Li recovery and no
179 induced isotope fractionation due to the purification process.

180 Accuracy and reproducibility of the entire method (purification procedure + mass analysis)
181 were tested by repeated measurements of a seawater sample (IRMM BCR-403) after
182 separation of Li from the matrix, for which we obtained a mean value of $\delta^7\text{Li} = +30.9\text{‰} \pm 0.4$
183 (2σ , 2 x Standard Deviation, $n = 12$) over the period of the duration of the analyses. This
184 mean value is in good agreement with our long-term measurement ($\delta^7\text{Li} = +31.0\text{‰} \pm 0.5$, 2σ ,
185 $n = 30$, Millot et al. 2004a) and with other values reported in the literature (see, for example,

186 Tomascak 2004 for a compilation). Consequently, based on long term measurements of the
187 seawater standard, we estimate the external reproducibility of our method to be around \pm
188 0.5‰ (2σ).

189 In addition, reproducibility of the method was also tested by repeated measurements of a
190 rainwater standard solution (TMRAIN-95, Environment Canada, National Water Research
191 Institute) after separation/purification by ion chromatography, for which we obtained a mean
192 value of $\delta^7\text{Li} = +445.9\text{‰} \pm 0.6$ (2σ , $n = 10$) over the period of the duration of the analyses.
193 This mean value could not, however, be compared either to literature data or to certified
194 values because this reference material is not certified for Li isotopes (only for Li
195 concentration). In spite of this, it is of interest to note that this rainwater standard solution is
196 significantly enriched in heavy lithium (^7Li). This is, however, not surprising because this
197 reference material is a synthetic rainwater solution (namely: *TMRAIN-95: a simulated rain*
198 *sample for trace elements*). Consequently, it is likely that lithium in this standard solution
199 could come from an ^7Li -rich reagent, as was pointed out by Qi et al. 1997, who showed that
200 $\delta^7\text{Li}$ values in laboratory reagents could range between -11 and +3013‰. Indeed, it is well
201 known that lithium can be isotopically fractionated due to the removal of ^6Li for use in
202 hydrogen bombs. The remaining lithium is therefore substantially enriched in ^7Li and some of
203 this lithium has found its way into laboratory reagents and into the environment (Coplen et al.
204 2002). In addition, we also measured an ICP ^7Li -rich standard solution (Spex) that has a
205 mean value of $\delta^7\text{Li} = +241.4\text{‰} \pm 0.5$ (2σ , $n = 38$, Millot et al. 2004b), which confirms the
206 results found by Qi et al. 1997.

207 Finally, concerning the lithium concentration of this rainwater standard solution (TMRAIN-95),
208 we obtained a good agreement between the values measured by ICP-MS in our laboratory
209 ($0.059 \mu\text{mol/L} \pm 0.003$, 2σ $n = 10$) and the certified value ($0.056 \mu\text{mol/L} \pm 0.011$).

210

211 **3.3. Boron isotopes**

212

213 Boron isotope composition were determined following a newly-developed methodology for
214 precise and accurate measurement using a Neptune double-focusing multi-collector sector
215 ICP-MS (Guerrot et al. 2010).

216 To avoid any drift of the mass bias induced by the sample matrix, chemical purification of 100
217 ng B was done before the mass analysis, following a procedure described in Guerrot et al.
218 (2010), using the specific boron resin IRA743 and 0.42N HNO_3 acid media with a final boron
219 concentration of 50 ng/mL. $^{11}\text{B}/^{10}\text{B}$ ratios were normalized, following the standard-sample
220 bracketing method, to the NIST SRM-951 standard solution (Catanzaro et al. 1970) run
221 through chemistry (Guerrot et al. 2010). Analytical uncertainty for each individual

222 determination was better than 0.1‰ at $2\sigma_m$ ($n = 20$). Accuracy and reproducibility of the
 223 whole process were determined by repeated measurements of a seawater solution (IAEA-
 224 B1) with a mean value of $\delta^{11}\text{B} = +39.36\text{‰} \pm 0.43$ (2σ , $n = 20$). This mean value is in good
 225 agreement with our measurements using the positive-TIMS- Cs_2BO_2 technique ($\delta^{11}\text{B} =$
 226 $+39.24\text{‰} \pm 0.36$ (2σ , $n = 19$), as well as with the data compilation obtained for an
 227 intercomparison exercise (Gonfiantini et al. 2003) and with the worldwide accepted value for
 228 seawater.

229 Consequently, based on long term measurements of seawater standards, we estimate the
 230 external reproducibility of our method around $\pm 0.5\text{‰}$ (2σ).

231

232 4. RESULTS AND COMMENTS

233

234 4.1. Stable isotopes of the water molecule: δD and $\delta^{18}\text{O}$

235

236 The main processes controlling the $\delta^{18}\text{O}$ and δD isotopic signatures in precipitations were
 237 summarized by Rozanski et al. (1993): i.e. the rainfall amount, continental and altitude
 238 effects and the origins of air masses. The morphology of France is complex with the Massif
 239 Central in the centre, the Alps to the East and the Pyrénées to the South, together with the
 240 influences of both the Atlantic Ocean and the Mediterranean Sea, which have very different
 241 characteristics, as evidenced by Celle-Jeanton et al. (2001) and Ladouche et al. (2009). It is,
 242 therefore, of primary importance to constrain the signature of the atmospheric signal in
 243 different geographical and geomorphological contexts by means of a rainfall-monitoring
 244 network.

245 The five monitoring stations (Brest, Dax, Orléans, Thonon and Avignon) were selected in
 246 order to have a good distribution over the national territory (Fig. 1). This enables, firstly, to
 247 follow the evolution of the isotopic signal over a West-East transect from Brest to Thonon via
 248 Orléans, and, secondly, to observe the influence of Mediterranean versus Atlantic air
 249 masses.

250 The equation of the Global Meteoric Water Line (GMWL) is $\delta\text{D} = 8 \times \delta^{18}\text{O} + 10$ (Craig 1961).
 251 The arithmetic (unweighted) means of isotopic ratios in precipitation from nearly 410 stations
 252 are described by the following equation: $\delta\text{D} = 8.07 (\pm 0.02) \times \delta^{18}\text{O} + 9.9 (\pm 0.1)$, $R^2 = 0.98$.
 253 Long-term means weighted by the amount of precipitation were calculated only for the year
 254 for which more than 70% of the rainfall was analysed and at least one year of observation
 255 was available (Gourcy et al. 2005). The correlation between the weighted means is: $\delta\text{D}_{\text{weighted}}$
 256 $= 8.14 (\pm 0.02) \times \delta^{18}\text{O} + 10.9 (\pm 0.2)$, $R^2 = 0.98$. When all the available data from the 5
 257 French monitoring stations are plotted in a $\delta^{18}\text{O}$ vs. δD diagram (Fig. 2a), the following

258 equation can be calculated: $\delta D = 7.727 (\pm 0.066) \times \delta^{18}O + 7.033 (\pm 0.451)$, $R^2 = 0.97$, $n =$
 259 411. When only annual weighted mean values are used for each monitoring station (Fig. 2b),
 260 the equation becomes: $\delta D = 8.347 (\pm 0.153) \times \delta^{18}O + 11.662 (\pm 1.048)$, $R^2 = 0.99$, $n = 31$.

261 These global results are close to the Global Meteoric Water Line despite the variability that
 262 can be found at each French station.

263 The weighted mean for each station integrates all the available data over the monitoring
 264 period. The Avignon weighted mean for the period 1997-2002, $\delta^{18}O = -5.81\%$, is similar to
 265 the one calculated during the 1997-1998 period, i.e. $\delta^{18}O = -6.1\%$ (Celle et al. 2000). These
 266 weighted means are reported in figure 3f, in which all points plot very close to the GMWL,
 267 and highlight the continental effect (also called the distance-from-the-coast-effect) with
 268 progressive depletion in heavy isotopes from Brest (Atlantic coast) to Thonon via Orléans
 269 (Fig. 1). It is worth noting that the best fit regression lines of the annual weighted means of
 270 these three stations described a quasi-straight line very close to the GMWL (Fig. 2b),
 271 suggesting a genetic link of rainfall for the three stations.

272 In greater detail, the continental effect can be assessed between Brest and Thonon samples
 273 (355 km apart) after removing the altitude effect for the Thonon station (at an altitude of 385
 274 m). Blavoux (1978) calculated an altitudinal gradient of $-0.3\%/100$ m in this region (Chablais,
 275 pre-Alpes), leading to a continental effect of $-3.2\% \delta^{18}O/1000$ km in an eastward direction
 276 from the French Atlantic Coast. This value is in good agreement with the assessment of
 277 Lécalle (1985) over the French territory. The continental effect varies considerably from place
 278 to place and from season to season (Ladouche et al. 2009), even over a low-relief profile. It
 279 is also strongly correlated with the temperature gradient and depends on both the
 280 topography and the climate regime.

281 Average annual $\delta^{18}O$ values vary from year to year (Fig. 2b). For the 5 French monitoring
 282 stations, the $\delta^{18}O$ values vary between 1 and 2‰ over the monitoring period, as was
 283 observed in Wallingford, UK (Darling and Talbot 2003). This is typical of temperate climates
 284 where a large part of the spread is caused by variations in the average annual temperature
 285 (Gat et al. 2001). These variations from year to year show why it is difficult to assess the real
 286 signature of precipitation in a given place without long-term monitoring. This should be kept
 287 in mind when drawing a contour map of $\delta^{18}O$ for a vast territory for which only a few long-
 288 term monitoring data are available.

289 **4.2. Lithium and boron concentrations in rainwaters**

291
 292 Major elements (cations and anions) and lithium and boron concentrations in rainwater
 293 samples collected in Brest, Dax, Orléans and Clermont-Ferrand are given in table 1. When
 294 Cl concentrations are plotted as a function of Na concentrations (Fig. 4, Négrel et al. 2007),

295 we observe a good correlation for the rainwater samples. The regression line between these
296 two major elements is also shown in figure 4. A 95% confidence level is assigned to the data
297 that falls between the two lines. The seawater dilution line is also shown in figure 4. Cl
298 concentrations show a very strong correlation with Na concentrations ($R^2 = 0.99$). All the
299 samples lie near the seawater dilution line, indicating that both the Na and Cl in these
300 samples come from sea salt. The Brest and the Dax rainwater samples have the highest Na
301 and Cl concentrations, whereas those collected near Clermont-Ferrand have the lowest
302 concentrations in both Na and Cl.

303 Lithium and boron concentrations in rainwater samples range from 0.004 to 0.292 $\mu\text{mol/L}$
304 and from 0.029 to 6.184 $\mu\text{mol/L}$, respectively. This range of variation for Li concentrations is
305 significantly lower than the only other value reported for rainwater (i.e. Li = 0.520 $\mu\text{mol/L}$, in
306 Hawaii, Pistiner and Henderson 2003). On the other hand, boron concentrations reported in
307 here are in agreement with literature data, with values sometimes higher in the present case
308 (Chetelat et al. 2005, Rose-Koga et al. 2006, Chetelat et al. 2009).

309 Li concentrations are more homogeneous than boron concentrations from one sampling site
310 to another. The mean lithium concentration values for the various sites are quite similar
311 (0.058, 0.066, 0.053 and 0.057 $\mu\text{mol/L}$ for rainwaters collected at Brest, Dax, Orléans and
312 near Clermont-Ferrand, respectively), whereas they are more heterogeneous for boron (i.e.
313 0.66, 0.90, 1.51 and 0.20 $\mu\text{mol/L}$ for rainwaters collected at Brest, Dax, Orléans and near
314 Clermont-Ferrand, respectively).

315 The overall range of variation for Li and B concentrations can be seen in figure 5a and 5b,
316 where lithium and boron concentrations are plotted as a function of the Na concentrations as
317 seasalt tracer (Négrel and Roy, 1998). Again, we see that these rainwater samples are rather
318 homogenous for lithium concentrations (with the exception of 2 Li-rich samples). Moreover, it
319 appears that rainwaters are slightly enriched in Li and B compared to Na derived from
320 seawater. No correlation could be found, however, between Li and B concentrations in
321 rainwater samples (Fig. 5c).

322

323 **4.3. Lithium and boron isotopes**

324

325 Lithium and boron isotope compositions are reported in table 1 and figure 6. The most
326 striking outcome of this study is that there is a very large range of variation (between +3.2
327 and +95.6‰) for $\delta^7\text{Li}$ in rainwaters. Mean $\delta^7\text{Li}$ values are +22.5, +22.8, +16.1 and +26.2‰ for
328 samples collected in Brest, Dax, Orléans and near Clermont-Ferrand, respectively. This
329 range of variation is consistent with the only other value reported for rainwater ($\delta^7\text{Li} =$

330 +14.3‰, in Hawaii, Pistiner and Henderson, 2003). Furthermore, $\delta^7\text{Li}$ values in rainwaters
331 are significantly different from the $\delta^7\text{Li}$ signature of seawater (+31‰, Millot et al. 2004a).

332 $\delta^{11}\text{B}$ in rainwaters also shows a very wide range of variation, between -3.3 and +40.6‰. The
333 mean $\delta^{11}\text{B}$ values are +37.4, +11.4, +8.4 and +23.2‰ for rainwaters collected in Brest, Dax,
334 Orléans and near Clermont-Ferrand, respectively. This is in agreement with literature data
335 (Chetelat et al. 2005, Rose-Koga et al. 2006, Chetelat et al. 2009) and is significantly
336 different from the $\delta^{11}\text{B}$ signature of seawater (+39.5‰, see data compilation reported by
337 Aggarwal et al. 2004), except for Brest.

338 In figures 7a and 7b, $\delta^7\text{Li}$ and $\delta^{11}\text{B}$ values are plotted as a function of Li and B
339 concentrations, respectively. No general correlation is observed between $\delta^7\text{Li}$ and Li
340 concentrations (Fig. 7a). Indeed, the range of $\delta^7\text{Li}$ variation is covered at both low and high Li
341 concentrations (with the exception of the three ^7Li -rich samples from Clermont-Ferrand). On
342 the other hand, there seems to be an inverse correlation between $\delta^{11}\text{B}$ and B concentrations
343 (Fig. 7b). Initially high $\delta^{11}\text{B}$ values (close to seawater signature, i.e. corresponding to
344 rainwater samples from Brest, which is near the ocean) tend to decrease down to nearly -3‰
345 as B concentrations increase. This also means that high B concentrations in rainwaters are
346 associated with low $\delta^{11}\text{B}$ values, especially for Orléans rainwater samples.

347 The overall range of variation for both $\delta^7\text{Li}$ and $\delta^{11}\text{B}$ values is very great (over 90‰ and 40‰,
348 respectively, for $\delta^7\text{Li}$ and $\delta^{11}\text{B}$, Fig. 6), and these isotopic signatures for rainwater samples
349 are significantly different from the isotopic signature of seawater (+31.0 and +39.5‰,
350 respectively, for $\delta^7\text{Li}$ and $\delta^{11}\text{B}$ values). Seawater might, therefore, be a major source of
351 dissolved atmospheric lithium and boron (especially for rainwater collected near the ocean),
352 but other sources must also be considered.

353

354

5. DISCUSSION

355

5.1. Contour map of the stable isotopic signature of oxygen ($\delta^{18}\text{O}$)

356

357
358 The world map developed by the IAEA from GNIP data (GNIP 2007) is one of the few
359 contour maps of the stable atmospheric signal that exist today. In France, a $\delta^{18}\text{O}$ contour
360 map was drawn by Lécolle (1985), based on the oxygen isotopic composition of the
361 carbonate shell of landsnails, which have been shown to be directly linked to the annual
362 mean $\delta^{18}\text{O}$ of rainwater. A second map, based on a few rainwater and groundwater
363 measurements, was drawn by Razafindrakoto (1988).

364 In the present work, the stations in Brest, Dax, Orléans, Avignon and Thonon (Fig. 1) were
365 monitored monthly for the $\delta^{18}\text{O}$ and δD atmospheric signal. Rain samples from the BDISO
366 databank are from studies dedicated to the knowledge and functioning of specific aquifers,
367 often represent only a few months of monitoring, and are not for the same time periods. From
368 all the available data, we selected data points with the following criteria: (1) there must be at
369 least one year of monitoring; (2) isotopic data should be associated with the rainfall amount
370 (if rainfall values are unavailable, data are weighted by those from the nearest meteorological
371 station at the same altitude); (3) when two points are close, only the longest and more recent
372 monitoring campaign is selected, as well as the lowest altitude point to minimize the altitude
373 effect when drawing the map. Rain data from 44 points were selected (Fig. 8). Some regions
374 are poorly documented and additional data were selected. In the Southwest of France, lakes
375 considered to be natural rain gages under well-defined conditions (lakes in pristine
376 environments located in the upper parts of drainage basins to limit runoff, Petelet-Giraud et
377 al. 2005) are used after data has been corrected for evaporation. Data from 13 lakes were
378 used. In other regions, recent groundwater (i.e. Tritium values >0 and ^{14}C Activity close to
379 100%) was used as a reference material as it has been shown to be often reasonably
380 representative of long-term rainfall (Darling et al. 2003). Data for 12 groundwater bodies
381 were used. No data are available for the Rhône River Valley. We, therefore, used a signature
382 calculated from that of a landsnail shell from the Northern part of the valley (Lécolle 1985).
383 To better determine the isotopic signature at the French border, we used data from the
384 literature or long-term rain monitoring data in the GNIP database for neighbouring countries
385 (GNIP 2007, Plata-Bedmar 1994, Longinelli and Selmo 2003, Longinelli et al. 2006, Darling
386 and Talbot 2003, Darling et al. 2003, Schurch et al. 2003).

387 The contour map of $\delta^{18}\text{O}$ values was drawn manually for the following reasons: (1) to take
388 into account the altitude from the topographic digital terrain model (DTM) for a better
389 interpolation, reflecting the altitude affect and (2) to give a greater weight to the most
390 representative samples (length of the monitoring campaign, altitude, etc.) when large isotopic
391 variations were observed at small scale. Our attempts to automatically generate the map with
392 dedicated software with kriging methods were rather inconclusive mainly because, as the
393 data including the altitude effect, it was impossible to take into account the DTM in the
394 interpolation without a risk of taking the altitude effect into account twice.

395 The resulting map of the meteoric $\delta^{18}\text{O}$ signal (Fig. 8) clearly shows the main effects that
396 could affect the isotopic signature of rainwater. The continental and altitude effects are
397 clearly visible. It is also in good agreement with the map drawn by Lécolle (1985), with a high
398 degree of precision, especially in the North. The new contour map still remains quite
399 schematic because of the limited number of available data points and the complexity of the
400 French topography. This is especially true in mountainous regions, where the density of data

401 is too low and the relief too uneven for us to draw reliable lines. $\delta^{18}\text{O}$ iso-value lines are,
402 therefore, represented by dotted lines in the Pyrénées and the Alps.

403 The map also shows that the signature along the Atlantic coast is relatively homogeneous
404 with a $\delta^{18}\text{O}$ value of around -5‰ , despite the difference in latitude and the known climatic
405 differences. The same phenomenon is observed on the Mediterranean coast of Italy
406 (Longinelli and Selmo 2003) and can be at least partially related to the contribution of
407 seawater vapor to the coastal precipitation, with values characteristic of a first condensate of
408 vapor (Gat et al. 2001). While the isotopic signal on the Mediterranean coast is not
409 significantly different from that on the Atlantic coast, the Mediterranean signature is more
410 rapidly depleted in heavy isotopes as we move inland from the coast. This could be due to
411 the presence of mountains close to the coast, which generate rainfall. Rainwater in and
412 around Paris is less depleted in heavy isotopes than available data indicates for the
413 surrounding area. This might be explained by a slightly higher temperature induced by the
414 high population density and intensive industrial activity. Such a phenomenon has been
415 described in Rome (Italy) (Longinelli and Selmo 2003). The Northern coast presents a $\delta^{18}\text{O}$
416 signal, depleted in heavy isotopes compared to the Atlantic coast (-6.5‰ vs. -5.3‰ in Brest
417 and -5.6‰ in Dax), which suggests that clouds that produce rainfall are already depleted in
418 heavy isotopes. This phenomenon has been observed over the British Isles. The $\delta^{18}\text{O}$
419 contour lines are parallel on each side of the Chanel.

420 This map is the first one drawn at the national scale based on most of the isotopic data
421 available in France, and which takes into account data for neighbouring countries in order to
422 better constrain the contour lines along the borders. It is, therefore, a unique tool for
423 assessing the stable isotopic signature of aquifer recharge for oxygen isotopes.
424 Nevertheless, it is worth noting that the rainwater data used often integrate only one year of
425 rainfall and we have shown that the mean annual weighted $\delta^{18}\text{O}$ values vary from 1 to 2‰
426 due to variations in the average annual temperature typical of temperate climates. This map
427 can, therefore, be a valuable addition to local rain monitoring when a specific aquifer is being
428 studied.

429 In this paper, we report only the $\delta^{18}\text{O}$ signature for France. However, δD can be determined
430 using the global correlation between δD and $\delta^{18}\text{O}$ (the Global Meteoric Water Line) since all
431 the data considered plot, for the most part, along this line.

432

433 **5.2. Lithium and boron isotopes variations**

434

435 *5.2.1. Seasonal and spatio-temporal variations*

436

437 Monitoring rainwater samples over a period of one year at different locations allows us to
438 study seasonal effects on the range of variation for both Li and B isotopes. We have plotted
439 Li and B isotopes as a function of the rainfall amount (mm) (Figs. 9a and b) and the month
440 (Figs. 9c and d). The rainfall amount seems to have no effect on $\delta^7\text{Li}$ variations (Fig. 9a). The
441 total range of variation for $\delta^7\text{Li}$ values seems to be independent of the rainfall amount, and
442 this is especially true for Orléans, Brest and Dax. On the other hand, for Brest and Dax
443 samples (sampling points on or near the coast), the rainfall amount does seem to control
444 $\delta^{11}\text{B}$ variations to some extent (Fig. 9b). When the rainfall amount increases, the $\delta^{11}\text{B}$ values
445 increase for the Brest samples but decrease for the Dax samples. It is very likely that when
446 the rainfall amount is great, there is a large contribution of sea salts derived from seawater.
447 This is especially true for the Brest rainwater samples (sampling point less than 5 km from
448 the Atlantic Ocean). However, the trend observed for $\delta^{11}\text{B}$ the rainwater samples from Dax
449 (30 km inland) is more complex. We know that, in this area, rainfall comes not only from the
450 Atlantic Ocean to the West, but also from the Pyrénées Mountains to the South. Therefore,
451 we can assume that for the Dax rainwater samples: (i) during the summer and winter (low
452 rainfall amount), $\delta^{11}\text{B}$ is controlled mainly by the sea salt contribution coming from the
453 Atlantic Ocean, whereas (ii) during spring and autumn when rainfall is heavier, $\delta^{11}\text{B}$ might
454 also be controlled by rain coming from the mountains that has been in contact with local dust
455 (i.e. silicate, carbonate and/or evaporite particulates from the Pyrénées), lowering $\delta^{11}\text{B}$
456 values. In addition, like Négrel et al. (2007) have observed for Sr isotopes at the same
457 sampling site, biogenic sources might also contribute to the $\delta^{11}\text{B}$ signature of the Dax
458 samples, also lowering the $\delta^{11}\text{B}$ values. Indeed, Dax is located in a huge maritime pine forest
459 (*Pinus pinaster*) that covers 860,000 hectares, the trees growing in sand containing chlorite,
460 micas, feldspars and quartz (Righi and De Connick 1977).

461 Rainwater samples from inland sampling points (Orléans and Clermont-Ferrand) do not show
462 any correlation of $\delta^{11}\text{B}$ values with the rainfall amount (Fig. 9b). Likewise, the month does not
463 appear to have any effect on $\delta^7\text{Li}$ values (Fig. 9c). However, ^7Li -rich values for Clermont-
464 Ferrand rainwater are observed during the winter and spring seasons (December, February
465 and April).

466 There appears to be no correlation between $\delta^{11}\text{B}$ values and the month (Fig. 9d). The range
467 of variation for $\delta^{11}\text{B}$ is controlled, first of all, by the location (inland vs. coastal) of the
468 sampling point.

469

470 *5.2.2. Wind direction and air mass origin*

471

472 The origin of the air masses for the French rainwater under consideration was studied using
473 the French Meteorological Institute database (www.meteofrance.com). Daily maximum wind
474 direction (0 to 360°) and rainfall (mm) were considered. Average monthly wind direction data
475 are given in table 1 for each sampling point. These average values were calculated by
476 weighting daily maximum wind directions by the corresponding rainfall amount and only rainy
477 days were considered.

478 The effect of wind direction, and thus the origin of the air masses, at each sampling site was
479 investigated by identifying correlations between wind direction and Li-B concentrations and
480 their isotopes.

481

482 *5.2.2.1. Lithium*

483

484 Li concentrations and $\delta^7\text{Li}$ values were plotted as a function of the wind direction (Fig. 10).
485 The wind direction does not control Li content in Brest and Clermont-Ferrand rainwater
486 samples (Figs. 10b and 10h). For Dax and Orléans sampling sites, however, there is a
487 correlation between Li concentration and wind direction (Figs. 10d and 10f). The lithium
488 concentration is controlled by the origin of the air masses for these rainwater samples, with
489 higher Li concentrations in rainwater coming from the ocean (wind direction around 270°, i.e.
490 W). Concerning $\delta^7\text{Li}$ values, no effect is observed, here again, for Brest rainwaters (Fig. 10a),
491 which means that most of rainwater at this site is homogeneous for both Li and its isotopes,
492 even though the wind direction can range significantly (from 50 to 240°, i.e., NE to WSW).
493 For Dax and Orléans samples, opposite phenomena are observed concerning Li isotopes.
494 When the air masses have a Western origin (oceanic input), $\delta^7\text{Li}$ values tend to increase
495 slightly for Dax rainwaters but decrease slightly for Orléans rainwaters (Figs. 10c and 10e).
496 The most striking observation concerns Clermont-Ferrand rainwaters, for which $\delta^7\text{Li}$ values
497 display two interesting trends as a function of the wind direction (Fig. 10g). In winter and
498 spring samples, there is a positive correlation between $\delta^7\text{Li}$ and wind direction. However,
499 autumn and summer samples show no change in the $\delta^7\text{Li}$ signature when the wind direction
500 is between 120 and 300°. This means that the ^7Li -rich rainwaters are characterized by air
501 masses coming from SSW of the sampling site during the winter and spring.

502

503 *5.2.2.2. Boron*

504

505 B concentrations and $\delta^{11}\text{B}$ values were plotted as a function of the wind direction (Fig. 11). B
506 concentrations in Brest and Clermont-Ferrand rainwaters are not controlled primarily by the
507 wind direction (Figs. 11b and 11h, respectively). However, for Dax and Orléans rainwaters, B

508 concentrations increase when the wind comes from West of the sampling site (marine origin,
509 Figs. 11d and 11f). There is no evidence that $\delta^{11}\text{B}$ values in Brest and Clermont-Ferrand
510 rainwaters are controlled by the wind direction (Figs. 11a and 11g), whereas $\delta^{11}\text{B}$ values in
511 Dax rainwaters increase when the wind direction ranges from 210° (SW) to 270° (W) (Fig.
512 11c), in agreement with our conclusions in section 5.2.1. concerning the two major origins of
513 boron at this site (sea salt from the Atlantic Ocean (W) and rainfall from the Pyrénées (SW)
514 having lower $\delta^{11}\text{B}$ values). $\delta^{11}\text{B}$ values in rainwater in Orléans decrease slightly when the
515 wind direction ranges from 180° (S) to 270° (W) (Fig. 11e).

516 The origin of the air masses is, therefore, an important factor that can control the dissolved
517 concentration of Li and B for the Dax and Orléans sampling sites, but seems to have no
518 effect on Clermont-Ferrand and Brest rainwaters. This is probably due to the homogeneity of
519 the rainfall for the Brest sampling site. On the other hand, for Dax, rainwater could have two
520 main origins – the SSW (with lower $\delta^7\text{Li}$ and $\delta^{11}\text{B}$ values) or the W (with higher $\delta^7\text{Li}$ and $\delta^{11}\text{B}$
521 values), which reflects the contribution of marine sea salts. For Clermont-Ferrand, the wind
522 direction has no significant effect on either Li or B concentrations, whereas we have seen
523 that the ^7Li -rich rainwaters are characterized by air masses coming from the SSW of the
524 sampling site during the winter and spring.

525 The spatial range of variation for Li and B isotopes could then be studied because we
526 monitored rainwater samples at different locations in France (coastal and inland). The
527 rainwaters sampled at Brest, near the sea, have both $\delta^7\text{Li}$ and $\delta^{11}\text{B}$ values close to the
528 seawater signature (Figs. 6 and 12), whereas those sampled at Dax, Orléans and Clermont-
529 Ferrand have a very broad range of variation for both $\delta^7\text{Li}$ and $\delta^{11}\text{B}$ values – from crustal
530 values (i.e. from -2 to +2‰ and from -5 to +10‰, respectively, for $\delta^7\text{Li}$ and $\delta^{11}\text{B}$, Teng et al.
531 2004, Tomascak 2004, Barth 1993, Barth 2000 and Millot et al. 2007) up to the $\delta^7\text{Li}$ and $\delta^{11}\text{B}$
532 signatures of seawater (+31.0 and +39.5‰, respectively, for $\delta^7\text{Li}$ and $\delta^{11}\text{B}$). However, higher
533 $\delta^7\text{Li}$ values are measured in some rainwater samples collected near Clermont-Ferrand. We,
534 therefore, discuss below the origins of lithium and boron in rainwaters, and the associated
535 isotope signatures, that might explain the observed range of variation for both Li and B
536 isotope systematics.

537

538 **5.3. Origin of lithium and boron in rainwaters**

539

540 Seawater (by contributing sea salts) might be one of the major suppliers of atmospheric
541 lithium and boron, but other sources must also to be taken into account. We, therefore,
542 determined the contribution of sea salts to lithium and boron in rainwater samples.

543 Na concentrations in rainwater samples can be used to estimate the sea salt contribution of
544 other ions because Na is the best tracer of sea salt input in rainwater (Keene et al. 1986,
545 Négrel and Roy 1998, Basak and Alagha 2004, Rastogi and Sarin 2005). Distinguishing
546 between the sea salt (ss) and non-sea salt (nss) component contributions in rainwater (rw) is
547 essential if we wish to characterize the chemistry of precipitation (Négrel and Roy 1998,
548 Schmitt and Stille 2005, Al-Khashman 2005, Rastogi and Sarin 2005, Négrel et al. 2007).
549 To calculate the contribution of Li and B (X in equation 1) in the sea salt component (ss) with
550 seawater (sw) characteristics, the following equation is used:

551

$$X_{ss} = Na_{rw} \times \left(\frac{X}{Na} \right)_{sw} \quad (1)$$

552

553

554 Na is used as a marine tracer in rainwater (see Négrel and Roy 1998 and references
555 therein). The contribution of the non-sea salt component (nss) is the difference between the
556 total composition of rainwater (rw) and the sea salt (ss) contribution:

$$X_{nss} = X_{rw} - X_{ss} \quad (2)$$

557

558

559 This equation enables us to determine the contribution of sea salts for lithium and boron
560 concentrations in rainwaters (Fig. 13). Results show that the contribution of sea salt for boron
561 concentrations in rainwaters is greater than for lithium concentrations. Indeed, considering
562 average values for the 4 different sampling sites, we see that the marine contribution (sea
563 salt) to B in rainwaters is twice that to Li (22.3% and 12.0%, respectively, Fig. 13). The
564 distance-from-the-coast-effect (inland vs. coastal location) is the key parameter controlling
565 the marine contribution for both Li and B to rainwater concentrations. Samples collected
566 inland (Orléans and Clermont-Ferrand) show the lowest sea salt contributions. Rainwaters
567 from Dax have intermediate values (Fig. 13), whereas rainwaters collected at Brest have the
568 highest contributions of marine sea salt to Li and B concentrations (25% and 49.8% on
569 average, respectively, for Li and B).

570 Although these results are not surprising, they show that although seawater does, indeed,
571 supply dissolved atmospheric lithium and boron, non sea salt sources represent the major
572 source of Li and B in rainwaters.

573 This could be of importance in hydrogeochemical studies of surface water and groundwater
574 bodies because rainwater is an input for the former and a recharge for the latter. The non
575 sea salt signature for Li and B isotopes should, therefore, be taken into consideration for
576 future studies in the investigation of their isotope systematics in water.

577

578 **5.4. Lithium isotopes in rainwaters**

579
580 The fact that most of dissolved Li in rainwaters does not have a marine origin is in agreement
581 with the range observed in $\delta^7\text{Li}$ in our samples (+3.2 and +95.6‰) compared to the marine
582 signature of Li isotopes ($\sim +31\%$).

583 $\delta^7\text{Li}$ values in rainwater samples were plotted as a function of Li derived from sea salt (Fig.
584 14a) in an attempt to identify the different sources contributing to the rainwaters Li isotopes
585 signature. For rainwater sampled at a coastal location (Brest), the marine contribution is
586 relatively great (9 to 45%), but another source or other sources is/are needed in order to
587 explain the range of variation in these $\delta^7\text{Li}$ values (+15.1 to +28.6‰). The same is observed
588 for rainwaters collected at Dax and Orléans, but at these locations the non sea salt
589 contribution should be even greater since these sites are located inland (especially Orléans)
590 and show lower marine contributions. The dissolution of either Li-bearing minerals or
591 anthropogenic inputs might explain lower $\delta^7\text{Li}$ values compared to the seawater signature (\sim
592 +31‰).

593 Continental rocks have $\delta^7\text{Li}$ values ranging from -4 to +8‰ (Teng et al. 2004 and references
594 therein) and might contribute to rainwater signatures by interaction in the atmosphere
595 between continental particles and water molecules. In addition, most carbonates analysed to
596 date show $\delta^7\text{Li}$ values between +6 and >25‰ (e.g. Hoefs and Sywall 1997, Hall et al. 2005,
597 Hathorne and James 2006, Vigier et al. 2007) and could also be cited there. It is, however,
598 more likely that multiple sources exist for the crustal component at the scale of France.

599 The three rainwater samples from Clermont-Ferrand having a ^7Li -rich signature ($\delta^7\text{Li}$ values
600 of +63.8, +77.6 and +95.6‰) are, however, notable because they have significantly heavier
601 Li isotopic compositions than seawater. Négrel and Roy (1998) and Roy and Négrel (2001)
602 have shown that rainwater in this area is likely to record an anthropogenic input due to
603 agricultural activities (e.g. fertilizers application). These high $\delta^7\text{Li}$ values might, therefore, be
604 explained by the contribution of a local input derived from fertilizers and/or soil amendments
605 used by farmers in this area. This is also in good agreement with recent results of Négrel et
606 al. (2009) concerning the Li isotopic characterization of a peat bog located near our sampling
607 site. In this study, the ^7Li -rich contribution to surface waters is explained by the dissolution of
608 fertilizers and soil amendments having $\delta^7\text{Li}$ values higher than +215‰ (Négrel et al. 2009).
609 This heavy lithium component is attributed to synthetic Li added into fertilizers and soil
610 amendments, derived from a ^7Li -rich reagent, as was reported by Qi et al. (1997). In addition,
611 we have seen (section 5.2.2) that these ^7Li -rich rainwaters are characterized by air masses
612 coming from the SSW of the sampling site during the winter and spring, which is when soils
613 are fertilized and amended.

614 When Li isotopes are plotted as a function of the Na/Li molar ratio (Fig. 15), we observe that
615 samples from Clermont-Ferrand seem to indicate a mixing of a crustal component (granite
616 and/or carbonate) and an anthropogenic component (^7Li -rich end-member), whereas
617 samples from Brest, Dax and Orléans seem to indicate a mixing of a crustal component
618 (complex due to the relative contribution of different particles derived from carbonate or
619 granite) and a marine end-member.

620

621 **5.5. Boron isotopes in rainwaters**

622

623 As stated above, most of the dissolved B in rainwater is not of marine origin (for rainwater
624 samples collected at inland locations in Orléans and Clermont-Ferrand, in particular). This is
625 in agreement with the range observed in $\delta^{11}\text{B}$ values in our samples (-3.3 and +40.6‰)
626 compared to the marine signature of B isotopes (+39.5‰, Aggarwal et al. 2004 and data
627 therein).

628 $\delta^{11}\text{B}$ values in rainwater samples have been plotted as a function of B derived from sea salt
629 (Fig. 14b). Seawater seems, nevertheless, to be a major supplier of rainwater boron in Brest,
630 near the ocean. However, the rainwater sample collected at Brest in August 2003 is notable
631 (the lowest $\delta^{11}\text{B}$ value: +27.5‰). It was collected at a time when France and Western Europe
632 were having an exceptionally severe heat wave with record temperatures and little rainfall
633 (Luterbacher et al. 2004, Chase et al. 2006), and it is very likely that this sample is not
634 representative.

635 Concerning the Dax, Orléans and Clermont-Ferrand rainwater samples, another source or
636 other sources is/are needed in order to explain the range of variation in $\delta^{11}\text{B}$ values. As for
637 lithium, the dissolution of either B-bearing minerals or anthropogenic inputs might explain
638 $\delta^{11}\text{B}$ values lower than the seawater signature (+39.5‰). A crustal component probably
639 contributes to rainwater signatures by the interaction in the atmosphere of continental
640 particles and water molecules. B isotopic compositions for the main crustal lithologies have
641 been well identified, with $\delta^{11}\text{B}$ values ranging from -5 to +10‰, from +15 to +30‰ and from 0
642 to +35‰, for granite and gneiss, marine evaporite and carbonate, respectively (Barth 1993,
643 2000). This crustal component is expected to contribute to the B isotopic rainwater signature,
644 although the crustal component is probably made up of a combination of several sources
645 (different particles coming from different lithologies).

646 Plotting B isotopic compositions as a function of NO_3/B molar ratios (NO_3 being a good tracer
647 of fertilizer) provides additional and important information (Fig. 16). Samples from Dax, for
648 which we have already suggested a possible biogenic input, are in agreement with field data
649 reported by Chetelat et al. (2005) for the biomass-derived end-member (this is also true for

650 most samples from Orléans, located near a large forested area, “La Sologne”, an area
651 covering 500,000 ha). In addition, the B values in rainwaters from this study are little affected
652 by anthropogenic emissions compared to those of rainwater sampled in Paris that have an
653 urban aerosol component (Chetelat et al. 2009). Most rainwater samples from Clermont-
654 Ferrand (for which we have cited a possible fertilizer input based on Li isotope data) also
655 reveal a mixing trend toward a fertilizer end-member (Fig. 16) based on B isotopes tracing.

656

657

6. CONCLUSIONS

658

659 This work has made it possible to better characterize Li, B, H and O isotopes in rainwaters.

660 The main results of this study are:

661 • Li and B concentrations and $\delta^7\text{Li}$ and $\delta^{11}\text{B}$ signatures in rainwater samples collected over
662 one year in four stations (Brest, Dax, Orléans and Clermont-Ferrand) varied greatly over the
663 sampling period.

664 • Lithium and boron concentrations are low and comprised between 0.004 and 0.292 $\mu\text{mol/L}$
665 and 0.029 and 6.184 $\mu\text{mol/L}$, respectively.

666 • $\delta^7\text{Li}$ and $\delta^{11}\text{B}$ values in rainwaters also vary greatly between +3.2 and +95.6‰ and -3.3 and
667 +40.6‰ over a period of one year, respectively.

668 • The seasonal effect (i.e. the month or rainfall amount) is not the main controlling factor for
669 these isotopic variations. However, the continental effect (distance from the coast) is a key
670 parameter, determining the origin of both lithium and boron derived from marine sea salts. In
671 addition, the origin of air masses (wind direction) is also a key parameter that controls the
672 contribution of sea salts derived from the Ocean.

673 • The most striking outcome of this study is that most lithium and boron in rainwaters does
674 not have a marine origin. Seawater is not the major supplier of atmospheric lithium and boron
675 and a non-sea-salt source, such as a crustal component and/or an anthropogenic
676 contribution, should also be taken into account when Li and B isotopes are studied in
677 hydrogeochemistry as an input to surface waters and a recharge to groundwater bodies. This
678 may be important in the understanding of dissolved Li and B distributions in ground- and
679 formation waters, and should be taken into account in future studies.

680 • A contour map of France for $\delta^{18}\text{O}$ was drawn after compiling data that included more than
681 400 values from all of France. This map could be used as a reference for future studies
682 concerning the recharge $\delta^{18}\text{O}$ signature in surface water and groundwater body
683 characterization. It represents a unique tool for assessing the stable isotopic signature of the
684 recharge of aquifers for oxygen isotopes.

685

686 **Acknowledgements**

687

688 This work was funded by the Research Division of the BRGM. The authors thank all the
689 people who have contributed to the French Isotopic Data Base (BDISO) through their
690 technical assistance, sampling and isotopic measurements: University of Paris-Sud (Orsay),
691 University of Avignon, Centre de Recherches Géodynamiques (Thonon-les-Bains), CEA
692 (Saclay) and BRGM in Orléans. BDISO aims at gathering isotopic data (mainly $\delta^{18}\text{O}$, δD , ^3H ,
693 ^{14}C , $\delta^{13}\text{C}$, $^{87}\text{Sr}/^{86}\text{Sr}$, $\delta^{11}\text{B}$ and $\delta^{15}\text{N}$) on French groundwater, surface water and rainwater. We
694 thank J. Garnier for compiling most of the $\delta^{18}\text{O}$ and δD data and drawing the first version of
695 the $\delta^{18}\text{O}$ contour map presented here. We thank Météo France (Direction de la Production)
696 for providing the wind direction and rainfall data. This work benefited from the collaboration of
697 BRGM's chemistry laboratories for major and trace element analyses: J.P. Ghestem, T.
698 Conte and C. Crouzet are thanked for their help, as well as C. Fléhoc for stable isotope
699 measurements (δD and $\delta^{18}\text{O}$). We also would like to thank M. Robert for her help in the
700 Neptune laboratory. This is BRGM contribution n° XXXX.

701

702

703

704

705

706 **References**

- 707
- 708 Aggarwal J.K., Mezger K., Pernicka E., Meixner A. (2004) The effect of instrumental mass
709 bias on $\delta^{11}\text{B}$ measurements: a comparison between thermal ionisation mass spectrometry
710 and multiple-collector ICP-MS. *International Journal of Mass Spectrometry*, 232: 259-263.
- 711 Al-Khashman O.A. (2005) Ionic composition of wet precipitation in the Petra Region, Jordan.
712 *Atmospheric Research*, 78: 1-12.
- 713 Barth S.R. (1993) Boron isotope variations in nature: a synthesis. *Geol. Rundsch*, 82: 640-
714 641.
- 715 Barth S.R. (2000) Geochemical and boron, oxygen and hydrogen isotopic constraints on the
716 origin of salinity in groundwaters from the crystalline basement of the Alpine Foreland.
717 *Applied Geochemistry*, 15: 937-952.
- 718 Basak B., Alagha O. (2004) The chemical composition of rainwater over Büyükçekmece
719 Lake, Istanbul. *Atmospheric Research*, 71: 275-288.
- 720 BDISO (2007) French Isotopic Data Base on groundwater, surface water and rainwater.
721 Available at: <http://infoterre.brgm.fr/eSIG/index.jsp>
- 722 Berner E.K., Berner R.A. (1987) The global water cycle. *Geochemistry and Environment*.
723 Prentice-Hall, 394 p.
- 724 Blavoux B. (1978) Etude du cycle de l'eau au moyen de l'oxygène 18 et du Tritium.
725 Possibilités et limites de la méthode des isotopes en milieu en hydrologie de la zone
726 tempérée. Thèse d'Etat, Université Paris VI, France.
- 727 Catanzaro E.J., Champion C.E., Garner E.L., Marinenko G., Sappenfield K.M., Shields W.R.
728 (1970) Standard reference materials: Boric acid; isotopic and assay standard reference
729 materials. US National Bureau of Standards, Special Publication 260-17, 70pp.
- 730 Celle H., Daniel M., Mudry J., Blavoux B. (2000) Signal pluie et traçage par les isotopes
731 stables en Méditerranée occidentale. Exemple de la région avignonnaise (Sud-Est de la
732 France). *Comptes Rendus de l'Académie des Sciences Paris*, 331: 647-650.
- 733 Celle-Jeanton H., Travi Y., Blavoux B. (2001) Isotopic typology of the precipitation in the
734 Western Mediterranean region at three different time scales. *Geophys. Res. Lett.*, 28:
735 1215-1218.
- 736 Chase T.N., Wolter K., Pielke R.A., Rasool I. (2006) Was the 2003 summer European heat
737 wave unusual in a global context? *Geophys. Res. Lett.*, 33: L23709.
- 738 Chetelat B., Gaillardet J., Freydier R., Négrel, Ph. (2005) Boron isotopes in precipitation:
739 experimental constraints and field evidence from French Guiana. *Earth Planet. Sci. Lett.*,
740 235: 16-30.
- 741 Chetelat B., Gaillardet J., Freydier R. (2009) Use of B isotopes as a tracer of anthropogenic
742 emissions in the atmosphere of Paris, France. *Applied Geochemistry* 24: 810-820.

743 Coplen T.B., Hopple J.A., Böhlke J.K., Peiser H.S., Rieder S.E., Krouse H.R., Rosman
744 K.J.R., Ding T., Vocke R.D.Jr., Révész K.M., Lamberty A., Taylor P., De Bièvre P. (2002)
745 Compilation of minimum and maximum isotope ratios of selected elements in naturally
746 occurring terrestrial materials and reagents. U.S. Geological Survey, Water-Resources
747 Investigations, Report 01-4222.

748 Craig H. (1961) Isotopic variations in meteoric waters. *Science*, 133: 1702-1703.

749 Darling W.G., Talbot J.C. (2003) The O and H stable isotopic composition of fresh waters in
750 the British Isles. 1. Rainfall. *Hydrology and Earth System Sciences*, 7: 163-181.

751 Darling W.G., Bath A.H., Talbot J.C. (2003) The O and H stable isotopic composition of fresh
752 waters in the British Isles. 2. Surface waters and groundwater. *Hydrology and Earth
753 System Sciences*, 7: 183-195.

754 Flesch G.D., Anderson A.R., Svec H.J. (1973) A secondary isotopic standard for $^6\text{Li}/^7\text{Li}$
755 determinations. *International Journal of Mass Spectrometry and Ion Physics*, 12: 265-272.

756 Gat J.R., Mook W.G., Meijer H.A.J. (2001) Volume II: Atmospheric Water. In: Mook, W.G.
757 (Eds), *Environmental Isotopes in the hydrological cycle. Principles and applications. IHP-V
758 Technical Documents in Hydrology*, N° 39. UNESCO-IAEA.

759 GNIP (2007) Global Network of Isotopes in Precipitation. Available at: <http://isohis.iaea.org/>

760 Gonfiantini R., Tonarini S., Gröning M., Adorni-Braccesi A., Al-Ammar A.S., Astner M.,
761 Bächler S., Barnes R.M., Bassett R.L., Cocherie A., Deyhle A., Dini A., Ferrara G.,
762 Gaillardet J., Grimm J., Guerrot C., Krähenbühl U., Layne G., Lemarchand D., Meixner A.,
763 Northington D.J., Pennisi M., Reitznerová E., Rodushkin I., Sugiura N., Surberg R., Tonn
764 S., Wiedenbeck M., Wunderli S., Xiao Y., Zack T. (2003) Intercomparison of boron isotope
765 and concentration measurements. Part II: Evaluation of results. *Geostandards Newsletter:
766 The Journal of Geostandards and Geoanalysis*, 27, 1: 41-57.

767 Gourcy L., Groening M., Aggarwal P.K. (2005) Stable oxygen and hydrogen isotopes in
768 precipitation. In: P.K., Aggarwal, J.R. Gat and K.F.O. Froehlich (eds), *Isotopes in the
769 Water Cycle: Past, Present and Future of the Developing Science*, 39-51.

770 Guerrot C., Millot R., Robert M., Négrel Ph. (2010) Accurate and high-precision
771 determination of boron isotopic ratio by MC-ICP-MS Neptune. *Geostandards and
772 Geoanalytical Research*, in revision.

773 Hall J.M. , Chan L.H., McDonough W.F., Turekian K.K. (2005) Determination of the lithium
774 isotopic composition of planktic foraminifera and its application as a paleo-seawater proxy.
775 *Marine Geology*, 217: 255-265.

776 Hathorne E.C., James R.H. (2006) Temporal record of lithium in seawater: A tracer for
777 silicate weathering? *Earth and Planetary Science Letters*, 246: 393-406.

- 778 Hoefs J., Sywall M. (1997) Lithium isotope composition of Quaternary biogene carbonates
779 and a global lithium isotope balance. *Geochimica et Cosmochimica Acta*, 61: 2679-2690.
- 780 James R.H., Palmer M.R. (2000) The lithium isotope composition of international rock
781 standards. *Chemical Geology*, 166: 319-326.
- 782 Junge C. E. (1963) *Air chemistry and radioactivity*. New York, Academic Press.
- 783 Keene W.C., Pszenny A.A.P., Galloway J., Hawley M.E. (1986) Sea-salt corrections and
784 interpretation of constituent ratios in marine precipitation. *Journal Geophysical Research*,
785 91: 6647-6658.
- 786 Ladouche B., Aquilina B., Dörfli N. (2009) Chemical and isotopic investigation of
787 rainwater in Southern France (1996-2002): Potential use as input signal for karst
788 functioning investigation. *Journal of Hydrology*, 367: 150-164.
- 789 Lécalle P. (1985) The oxygen isotope composition of landsnail shells as a climatic indicator:
790 applications to hydrogeology and paleoclimatology. *Chemical Geology*, 58: 157-181.
- 791 Longinelli A., Selmo E. (2003) Isotopic composition of precipitation in Italy: a first overall
792 map. *Journal of Hydrology*, 270 : 75-88.
- 793 Longinelli A., Anglesio E., Flora O., Iacumin P., Selmo E. (2006) Isotopic composition of
794 precipitation in Northern Italy: Reverse effect of anomalous climatic events. *Journal of*
795 *Hydrology*, 329: 471-476.
- 796 Luterbacher J., Dietrich D., Xoplaki E., Grosjean M., Wanner H. (2004) European seasonal
797 and annual temperature variability, trends, and extremes since 1500. *Science*, 303: 1499-
798 1503.
- 799 Millot R., Guerrot C., Vigier N. (2004a) Accurate and high precision measurement of lithium
800 isotopes in two reference materials by MC-ICP-MS. *Geostandards and Geoanalytical*
801 *Research*, 28: 53-159.
- 802 Millot R., C. Guerrot, T.D. Bullen (2004b) Precise measurement of Li isotopes by MC-ICP-
803 MS and comparison with TIMS analyses. Winter Conference on Plasma
804 Spectrochemistry, January 5-10, Fort Lauderdale, USA.
- 805 Millot R., Négrel Ph, Petelet-Giraud E (2007) Multi-isotopic (Li, B, Sr, Nd) approach for
806 geothermal reservoir characterization in the Limagne Basin (Massif Central, France)
807 *Applied Geochemistry*, 22: 2307-2325.
- 808 Miyata Y., Tokieda T., Amakawa H., Uematsu M., Nozaki, Y. (2000) Boron isotope variations
809 in the atmosphere. *Tellus* 52B, 1057-1065.
- 810 Négrel Ph., Lachassagne P., Laporte P. (1997) Caractérisation chimique et isotopique des
811 pluies de Cayenne (Guyane Française). *C.R. Académie des Sciences* 324, 379-386.
- 812 Négrel Ph., Roy, S. (1998) Chemistry of rainwater in the Massif Central (France) A Strontium
813 isotope and major element study, *Applied Geochemistry* 13: 941-952.

- 814 Négrel Ph., Guerrot C., Millot R. (2007) Chemical and strontium isotope characterization of
815 rainwater in France: influence of sources and hydrogeochemical implications. *Isotopes in*
816 *Environmental and Health Studies*, 43: 179-196.
- 817 Négrel Ph., Millot R., Brenot A. (2009) Lithium isotopes as a probe of groundwater circulation
818 in a peat land. 8th International Symposium on Applied Isotope Geochemistry, La Malbaie,
819 Canada.
- 820 Petelet-Giraud E., Casanova J., Chery L., Négrel Ph., Bushaert S. (2005) Attempt of isotopic
821 characterisation (δ O-18 and δ H-2) of present rainwater signature using lakes and
822 reservoirs: application to south-western France. *Houille Blanche-Revue Internationale de*
823 *l'Eau*, 2: 57-62.
- 824 Pistiner J.S., Henderson G.M. (2003) Lithium isotope fractionation during continental
825 weathering processes. *Earth and Planetary Science Letters*, 214: 327-339.
- 826 Plata-Bedmar A. (1994) Composicion isotopica de las precipitaciones y aguas subterraneas
827 de la Peninsula Iberica. Centro des Estudios de tecnicas Aplicadas, Madrid (Spain), 139p.
- 828 Pogge von Strandmann P.A.E., Burton K.W., James R.H., van Calsteren P., Gislason S.R.,
829 Mokadem F. (2006) Riverine behaviour of uranium and lithium isotopes in an actively
830 glaciated basaltic terrain. *Earth and Planetary Science Letters*, 251: 134-147.
- 831 Qi H.P., Coplen T.B., Wang Q.Z., Wang Y.H. (1997) Unnatural isotopic composition of lithium
832 reagents. *Analytical Chemistry*, 69: 4076-4078.
- 833 Rastogi N., Sarin M.M. (2005) Chemical characteristics of individual rain events from a semi-
834 arid region in India: Three-year study. *Atmospheric Environment*, 39: 3313-3323.
- 835 Razafindrakoto S. (1988) Teneurs en isotopes stables des précipitations et des eaux
836 souterraines et leurs variations en France. PhD Thesis, Université d'Avignon et des Pays
837 de Vaucluse, 341p.
- 838 Righi D., De Connick F. (1977) Mineralogic evolution in hydromorphic sandy soils and
839 podzols in "Landes du médoc", France. *Geoderma*, 19: 339-359.
- 840 Rozanski K., Araguas-Araguas L., Gonfiantini R. (1993) Isotopic patterns in modern global
841 precipitation. In *Climate Change in Continental Isotopic Records*. Geophysical Monograph
842 78, American Geophysical Union.
- 843 Rose-Koga E.F., Sheppard S.M.F., Chaussidon M., Carignan J. (2006) Boron isotopic
844 composition of atmospheric precipitations and liquid-vapor fractionations. *Geochim.*
845 *Cosmochim. Acta*, 70: 1603-1615.
- 846 Roy .S, Négrel Ph. (2001) A Pb isotope and trace element study of rainwater from the Massif
847 Central (France). *Science of the Total Environment*, 277, 225-239.
- 848 Schmitt A.D. Stille P. (2005) The source of calcium in wet anthropogenic deposit: Ca-Sr
849 isotope evidence, *Geochimica et Cosmochimica Acta*, 69: 3463-3468.

- 850 Schurch M., Kozel R., Schotterer U., Tripet J.P. (2003) Observation of isotopes in the water
851 cycle - the Swiss National Network (NISOT). *Environmental Geology*, 45: 1-11.
- 852 Teng F.Z., McDonough W.F., Rudnick R.L., Dalpé C., Tomascak P.B., Chappell B.W., Gao
853 S. (2004) Lithium isotopic composition and concentration of the upper continental crust.
854 *Geochimica et Cosmochimica Acta*, 68: 4167-4178.
- 855 Tomascak P.B. (2004) Developments in the Understanding and Application of Lithium
856 Isotopes in the Earth and Planetary Sciences. In *Reviews in Mineralogy & Geochemistry*,
857 55: 153-195.
- 858 Vigier N., Rollion-Bard C., Spezzaferri S., Brunet F. (2007) In-situ measurements of Li
859 isotopes in foraminifera. *Geochemistry, Geophysics, Geosystems* Q01003.
- 860 Widory D., Petelet-Giraud E., Négrel Ph., Ladouche B. (2005) Tracking the sources of nitrate
861 in groundwater using coupled nitrogen and boron isotopes: A synthesis. *Environmental*
862 *Science & Technology*, 39: 539-548.
- 863

864 **Table caption**

865

866 **Table 1**

867 Major cations and anions (Na, K, Mg, Ca, Cl, SO₄, NO₃, μmol/L), Li and B concentrations
868 (μmol/L) and Li and B isotope compositions of rainwaters by location and sampling date.
869 Rainfall amount (mm) and wind direction are also reported in this table. The prevailing wind
870 direction data (in °) at each sample location were obtained from the Météo France database.
871 Data reported for monthly average values in this table are weighted by the rainfall amount
872 and only days with precipitation are considered.

873

874

875 **Figure captions**

876

877 **Figure 1**

878 Map of the rainwater sampling sites for lithium and boron isotopes (Brest, Dax, Orléans and
879 Clermont-Ferrand). Graphs show the monthly mean rainfall amount (mm) at each site
880 (modified from Négrel et al. 2007). Long-term monitoring stations for hydrogen and oxygen
881 isotopes of the water molecule, at Thonon and Avignon, are also shown on this map.

882

883 **Figure 2**

884 2a: $\delta^{18}\text{O}$ vs. δD for all the monthly samples from the 5 long-term monitoring stations (Orléans,
885 Brest, Dax, Thonon and Avignon. 2b: Annual weighted means of the same 5 stations. The
886 Global Meteoric Water Line is also drawn (GMWL, $\delta\text{D} = 8 \times \delta^{18}\text{O} + 10$).

887

888 **Figure 3**

889 3a to 3e: $\delta^{18}\text{O}$ vs. δD for the monthly samples for each station. 3f: Mean weighted values for
890 the period considered at each station. Blue diamonds correspond to individual data, red stars
891 are the weight mean values and the grey dashed line is the Global Meteoric Water Line
892 (GMWL) is $\delta\text{D} = 8 \times \delta^{18}\text{O} + 10$.

893

894 **Figure 4**

895 Cl concentrations in rainwaters ($\mu\text{mol/L}$) plotted as a function of the Na concentrations in
896 rainwaters ($\mu\text{mol/L}$). The seawater dilution line and the linear relationship between Cl and Na
897 are represented. A 95% confidence level is assigned to the data that falls between the two
898 lines (modified from Négrel et al. 2007).

899

900 **Figure 5**

901 5a and 5b: Lithium and boron concentrations in rainwaters ($\mu\text{mol/L}$) vs. sodium
902 concentrations in rainwaters ($\mu\text{mol/L}$). 5c: Lithium concentrations in rainwaters ($\mu\text{mol/L}$)
903 plotted as a function of boron concentrations in rainwaters ($\mu\text{mol/L}$).

904

905 **Figure 6**

906 Histograms for $\delta^7\text{Li}$ and $\delta^{11}\text{B}$ (‰) values in rainwater samples.

907

908 **Figure 7**

909 7a and 7b: $\delta^7\text{Li}$ and $\delta^{11}\text{B}$ (‰) values plotted as a function of lithium and boron concentrations,
910 respectively, in rainwaters ($\mu\text{mol/L}$).

911

912 **Figure 8**

913 Isovalue contour lines of the mean annual oxygen isotopic composition ($\delta^{18}\text{O}$) of rainwater in
914 France. This map is based on rainwater, groundwater, lake (corrected for evaporation) and
915 landsnail shell data. Contour lines from Spain (Plata-Bedmar 1994), Italy (Longinelli and
916 Selmo 2003, Longinelli et al. 2006) and United Kingdom (Darling and Talbot 2003, Darling et
917 al. 2003), together with Swiss data (Schurch et al. 2003) where also used to constrain lines
918 at the French borders. The location of rainwater sampling stations for $\delta^{18}\text{O}$ vs. δD is also
919 shown on this map (blue: short-term monitoring; red: long-term monitoring).

920

921 **Figure 9**

922 9a and 9b: $\delta^7\text{Li}$ and $\delta^{11}\text{B}$ (‰) values plotted as a function of rainfall amount (mm); 9c and 9d:
923 and sampling month.

924

925 **Figure 10**

926 $\delta^7\text{Li}$ (‰) values and Li concentrations ($\mu\text{mol/L}$) plotted as a function of wind direction for each
927 sampling site. Bold lines represent parameter trends as a function of wind direction.

928

929 **Figure 11**

930 $\delta^{11}\text{B}$ (‰) values and B concentrations ($\mu\text{mol/L}$) plotted as a function of wind direction for
931 each sampling site. Bold lines represent parameter trends as a function of wind direction.

932

933 **Figure 12**

934 $\delta^7\text{Li}$ (‰) plotted as a function of $\delta^{11}\text{B}$ (‰) in rainwater samples.

935

936 **Figure 13**

937 Histograms for Li and B contribution of marine sea salts (%) in rainwater samples.

938

939 **Figure 14**

940 14a and 14b: Li and B isotopic compositions plotted as a function of Li and B contribution of
941 marine sea salts in rainwater samples, respectively.

942

943 **Figure 15**

944 $\delta^7\text{Li}$ (‰) plotted as a function of the Na/Li molar ratio.

945

946 **Figure 16**

947 $\delta^{11}\text{B}$ (‰) plotted as a function of NO_3/B molar ratios. The anthropogenic end-member (urban
948 aerosols) is from Chetelat et al. (2009), the biomass-derived end-member is from Chetelat et
949 al. (2005) and the fertilizer end-member is from Widory (pers. comm.).
950

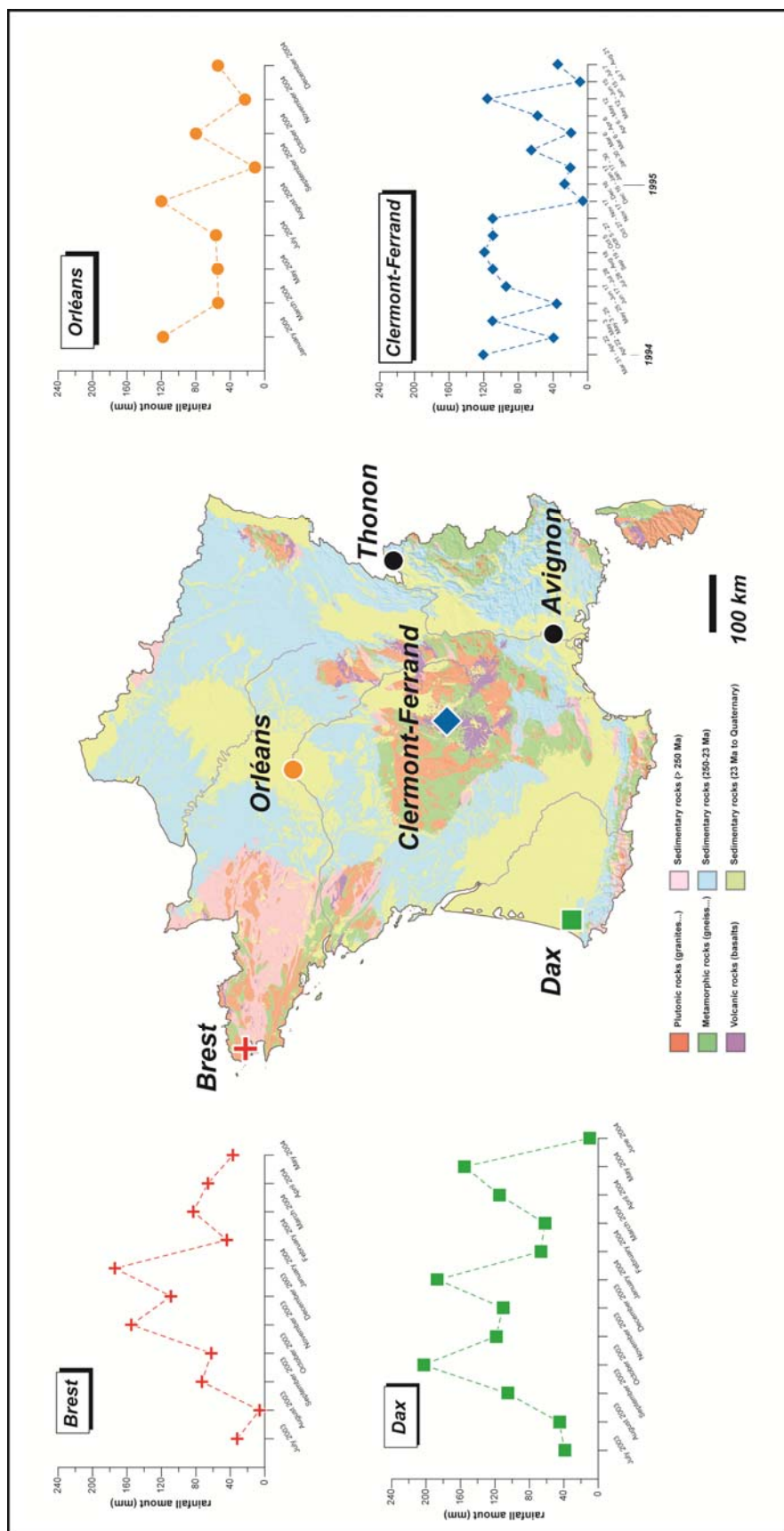
951
952
953
954

Table 1

955
956

Location / Sampling date	Reference	Rainfall amount mm	Main Wind direction °	Na μmol/L	K μmol/L	Mg μmol/L	Ca μmol/L	Cl μmol/L	SO ₄ μmol/L	NO ₃ μmol/L	Li μmol/L	B μmol/L	δ ¹³ C ‰	δ ¹⁵ N ‰	δ ¹⁸ O ‰
BREST															
July 2003	03-E-524	32	223	117.5	5.8	16.1	8.5	117.7	21.3	36.7	0.051	0.398	23.4	35.1	
August 2003	03-E-525	6	105	235.0	31.9	62.8	65.8	228.6	113.9	172.0	0.142	3.793	19.3	27.5	
September 2003	03-E-526	73	176	74.3	2.8	10.9	7.9	75.2	22.3	68.9	0.051	0.262	15.1	38.1	
October 2003	03-E-527	62	193	208.3	5.6	23.8	11.4	218.9	32.2	58.9	0.052	0.329	22.2	39.6	
November 2003	03-E-528	155	129	142.6	10.2	17.2	6.0	150.1	23.2	10.2	0.053	0.207	17.7	40.3	
December 2003	03-E-529	109	174	292.7	7.6	33.1	6.2	322.3	31.3	32.1	0.060	0.298	27.2	40.6	
January 2004	04-E-52	174	232	231.7	5.1	25.7	7.0	243.1	25.5	6.8	0.050	0.214	28.6	40.1	
February 2004	04-E-53	44	57	393.8	10.3	47.8	15.9	450.1	46.0	36.0	0.059	0.355	26.3	37.8	
March 2004	04-E-54	83	209	346.2	11.0	40.6	12.6	390.4	42.3	47.0	0.042	0.449	25.8	39.5	
April 2004	04-E-55	66	150	227.7	4.8	27.6	10.2	236.3	39.3	57.8	0.033	0.357	22.7	37.5	
May 2004	04-E-56	37	234	323.9	10.7	39.5	12.6	366.2	42.1	80.3	0.045	0.599	19.4	35.2	
DAX															
July 2003	03-E-164	39	256	204.3	63.6	24.4	55.2	156.6	43.9		0.069	1.013	34.1	15.9	
August 2003	03-E-165	45.4	248	89.5	9.2	14.9	33.8	50.7	40.8	49.7	0.078	1.167	21.5	7.9	
September 2003	03-E-166	105.4	225	196.1	14.3	18.0	23.2	176.3	32.5	2.6	0.067	0.717	21.1	12.9	
October 2003	03-E-147	203.1	207	273.6	50.2	26.9	57.8	272.3	33.8	110.6	0.077	1.174	25.2	8.3	
November 2003	03-E-148	118.7	238	155.7	15.9	15.2	25.7	136.6	24.8	-	0.062	0.830	19.8	2.0	
December 2003	03-E-149	110.7	230	194.2	11.5	16.9	44.6	167.0	30.6	2.9	0.058	0.595	21.0	11.8	
January 2004	03-E-150	187.3	242	176.4	9.3	16.9	20.8	164.8	25.9	-	0.047	0.997	23.0	7.1	
February 2004	03-E-151	66.8	212	203.9	51.0	29.6	49.2	198.3	44.9	28.7	0.058	0.369	23.5	19.8	
March 2004	03-E-152	62.1	210	137.4	41.9	27.1	64.5	135.5	36.9	3.5	0.055	0.662	17.2	9.4	
April 2004	03-E-153	115.1	255	255.2	53.8	33.7	65.0	247.3	18.3	3.0	0.068	1.099	18.9	7.9	
May 2004	03-E-154	155.1	243	160.1	10.9	19.8	31.4	163.7	23.5	-	0.050	0.898	22.8	7.8	
June 2004	03-E-155	10.2	268	108.3	26.8	22.8	114.4	113.5	42.0	-	0.079	1.340	25.3	26.5	
ORLEANS															
January 2004	04-E-46	118	221	38.7	6.9	5.8	8.9	32.7	8.4	-	0.041	0.029	13.0	29.8	
March 2004	04-E-48	54	231	61.4	11.3	10.8	21.4	49.6	22.6	39.4	0.055	0.408	14.2	13.1	
May 2004	04-E-50	55	243	52.4	17.0	8.2	12.7	39.4	14.1	9.5	0.046	0.818	19.2	6.0	
July 2004	04-E-295	57	220	53.4	13.5	12.0	23.3	30.4	21.0	-	0.068	1.987	11.2	-0.3	
August 2004	04-E-296	120	267	34.5	6.6	11.6	21.0	16.6	14.0	-	0.057	2.430	9.2	-2.4	
September 2004	04-E-297	11.5	234	96.9	19.4	22.8	39.4	98.3	27.9	-	0.081	6.184	19.4	-3.3	
October 2004	04-E-298	80	175	59.0	14.4	8.9	12.9	41.7	16.5	12.9	0.038	1.246	14.3	0.0	
November 2004	04-E-299	23	219	92.3	60.5	13.3	17.8	66.8	39.5	59.0	0.052	0.281	22.9	22.7	
December 2004	04-E-300	54	201	51.0	17.8	6.3	9.4	50.1	13.0	19.8	0.036	0.217	21.9	9.8	
CLERMONT-FERRAND															
March 31 - April 22 1994	PSM1	120	288	39.1	4.1	4.4	12.3	39.4	51.0	74.6	0.049	0.312	77.6	11.9	
April 22 - May 3 1994	PSM2	40	173	6.1	4.1	2.1	10.5	7.0	23.4	16.7	0.041	0.156	6.7	22.9	
May 3 - 25 1994	PSM3	110	239	3.9	2.6	1.7	8.0	7.0	16.1	34.1	0.004	0.116	8.7	28.7	
May 25 - June 17 1994	PSM4	37	256	9.1	7.2	0.2	14.8	16.9	19.8	-	0.075	0.191	4.9	25.0	
June 17 - July 28 1994	PSM5	95	256	20.0	23.8	4.3	79.0	31.0	47.9	42.9	-	-	-	-	
July 28 - August 18 1994	PSM6	110	243	4.8	3.3	0.9	16.8	16.9	33.3	30.2	0.033	0.248	6.7	32.8	
September 19 - October 5 1994	PSM7	120	294	4.3	2.3	1.9	16.8	7.9	7.1	12.7	0.027	0.106	9.0	32.0	
October 5 - 27 1994	PSM8	110	152	8.7	2.6	0.8	15.0	10.1	7.3	-	0.027	0.050	14.7	19.5	
October 27 - November 17 1994	PSM9	110	172	0.4	13.6	6.3	1.0	13.5	4.2	-	-	-	-	-	
November 17 - December 16 1994	PSM10	5	246	6.5	3.8	6.3	9.5	13.0	36.6	53.8	-	-	-	-	
December 16 1994 - January 17 1995	PSM11	28	197	32.2	1.8	8.3	12.0	44.2	21.6	38.7	0.044	0.172	63.8	27.2	
January 17 - 30 1995	PSM12	20	195	8.7	3.1	5.8	3.3	14.1	6.1	-	0.041	0.104	33.2	25.4	
January 30 - March 6 1995	PSM13	65	214	43.0	2.3	4.0	5.8	21.7	13.2	19.0	0.292	0.520	95.6	4.8	
March 6 - April 6 1995	PSM14	20	208	23.0	5.1	3.2	12.3	25.4	14.2	17.5	-	-	-	-	
April 6 - May 12 1995	PSM15	58	352	8.3	4.1	2.3	11.0	11.8	39.4	47.0	0.022	0.160	3.2	19.8	
May 12 - June 15 1995	PSM16	115	229	8.7	4.9	2.6	18.0	-	-	-	0.044	0.226	7.8	25.2	
June 15 - July 7 1995	PSM17	10	124	4.8	9.0	-	12.0	37.5	13.9	69.2	0.037	0.239	8.3	26.8	

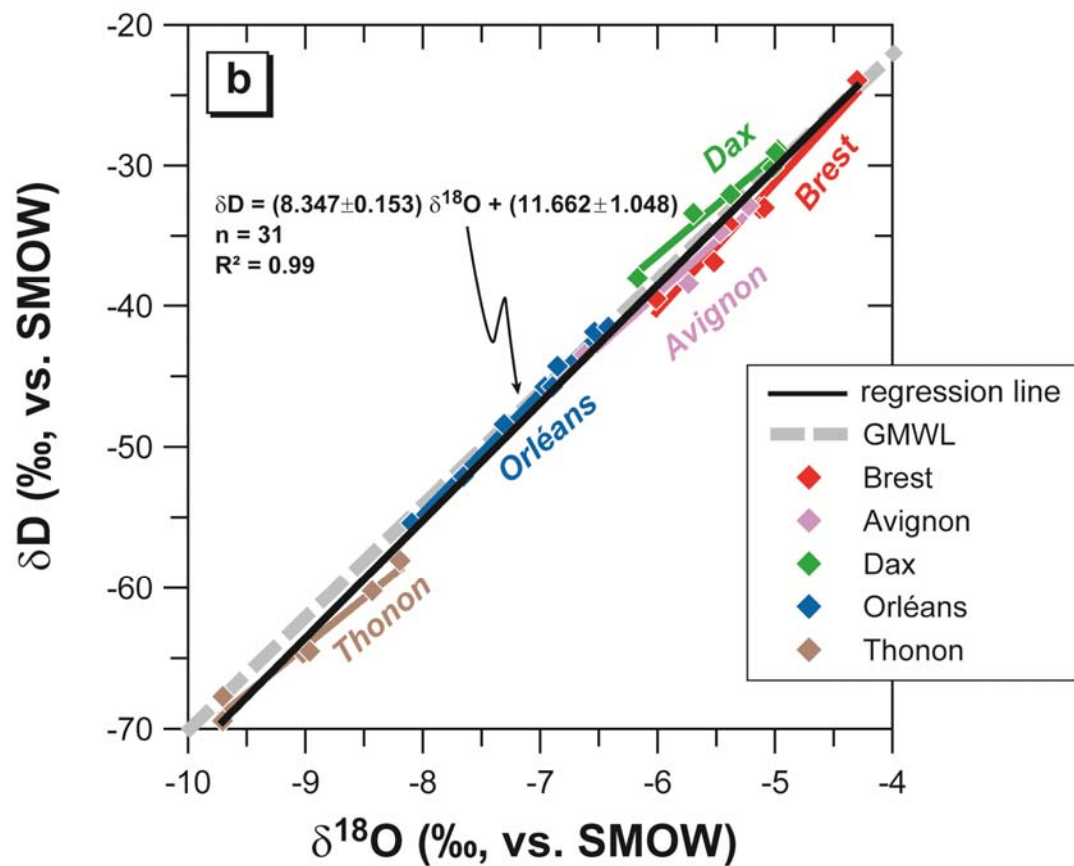
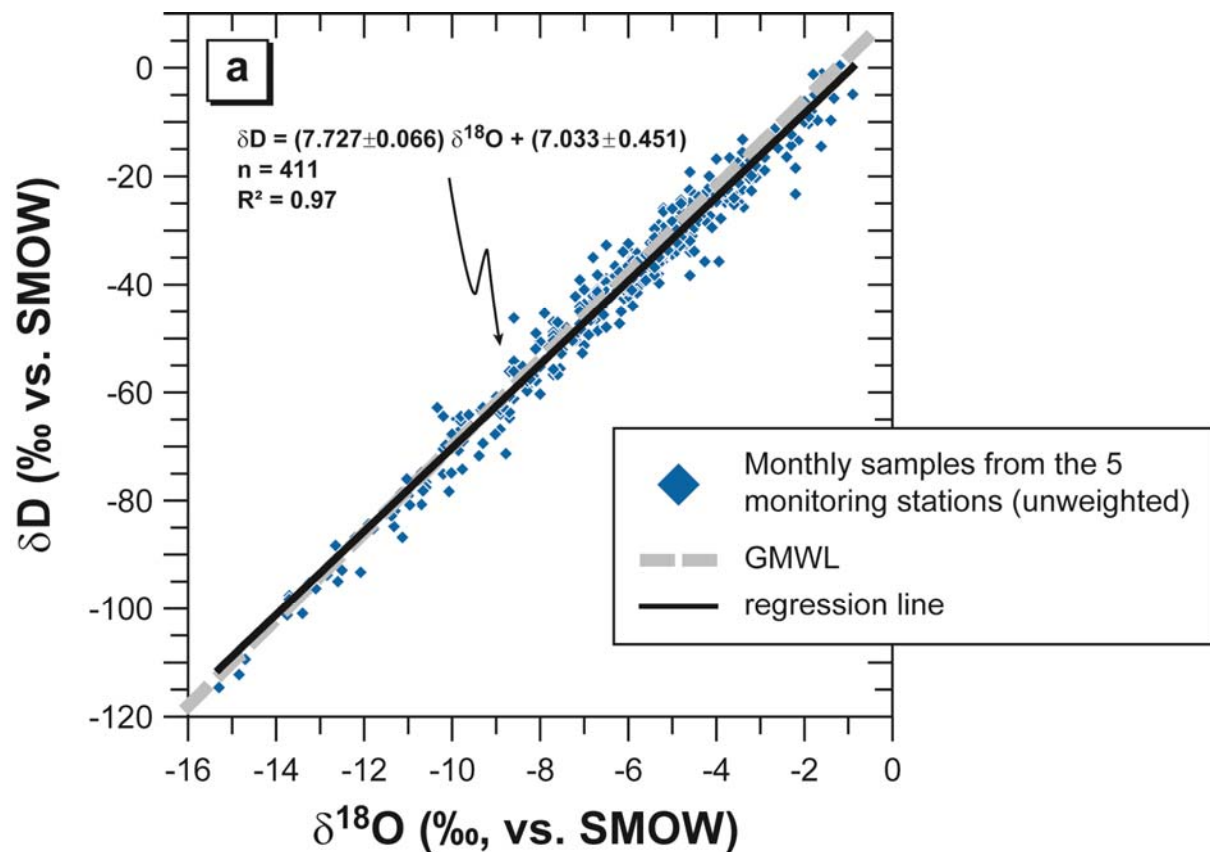
957 **Figure 1**
958



959

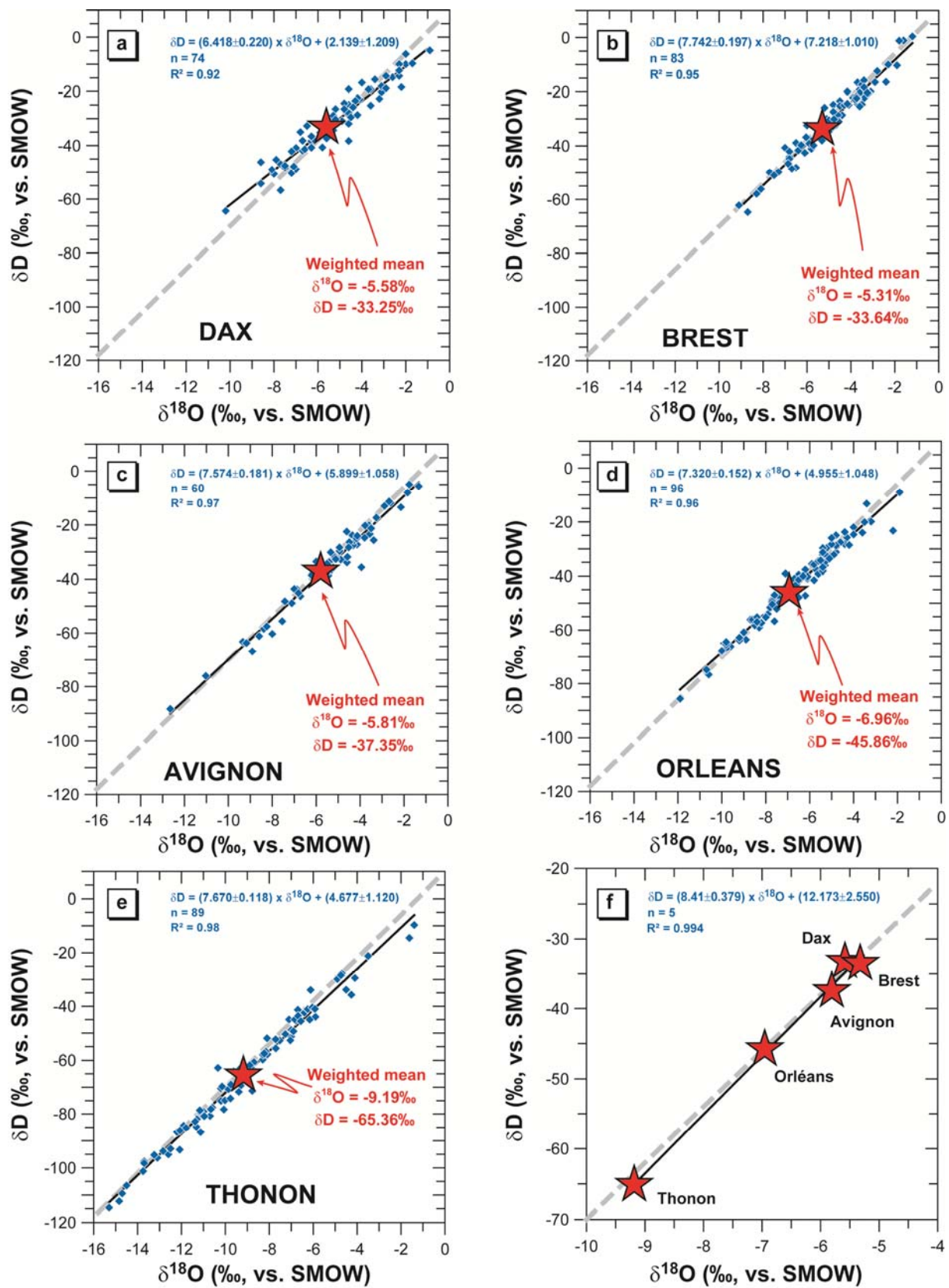
960
961

Figure 2



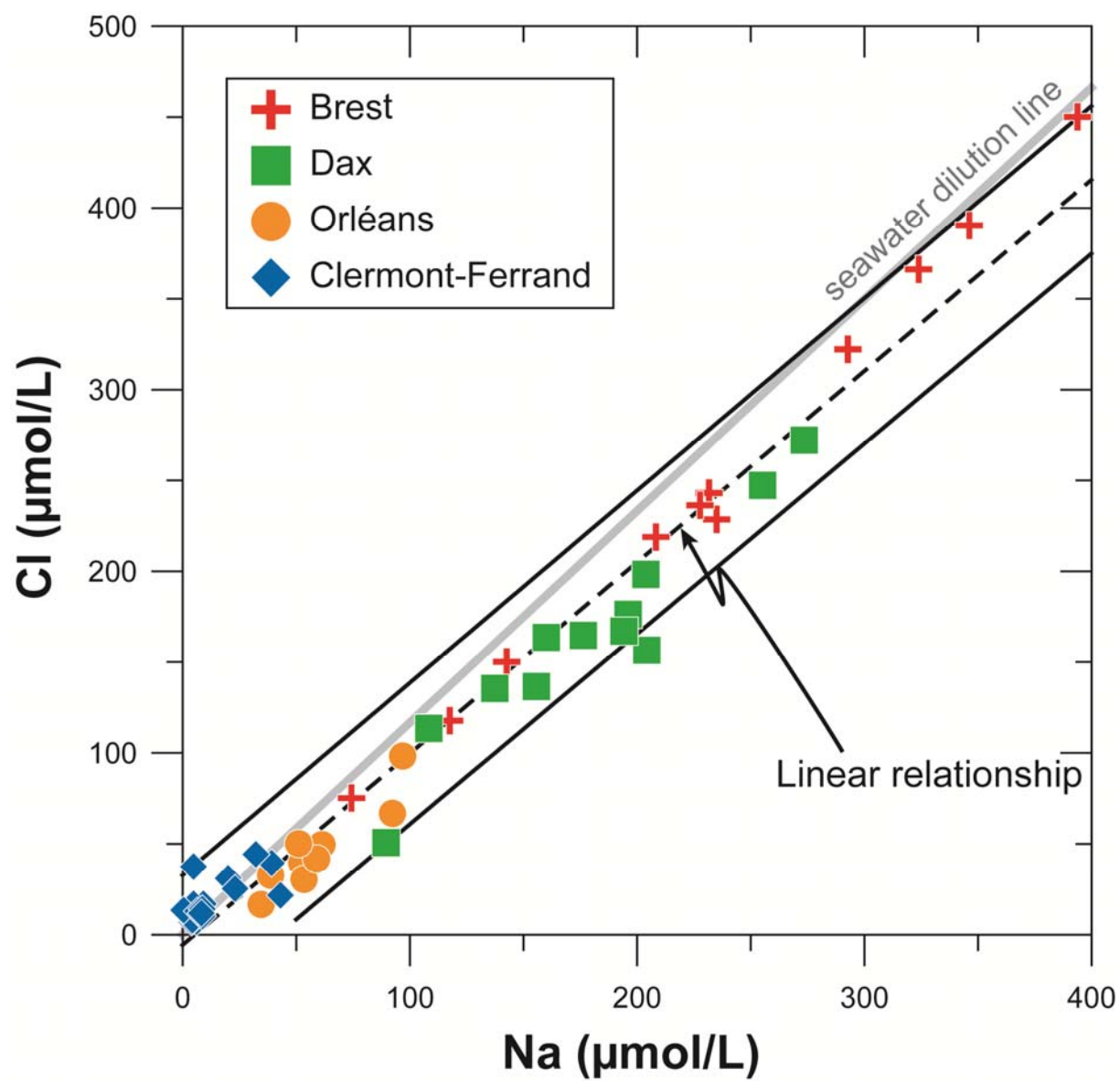
962

Figure 3



966
967
968
969
970
971
972
973
974
975

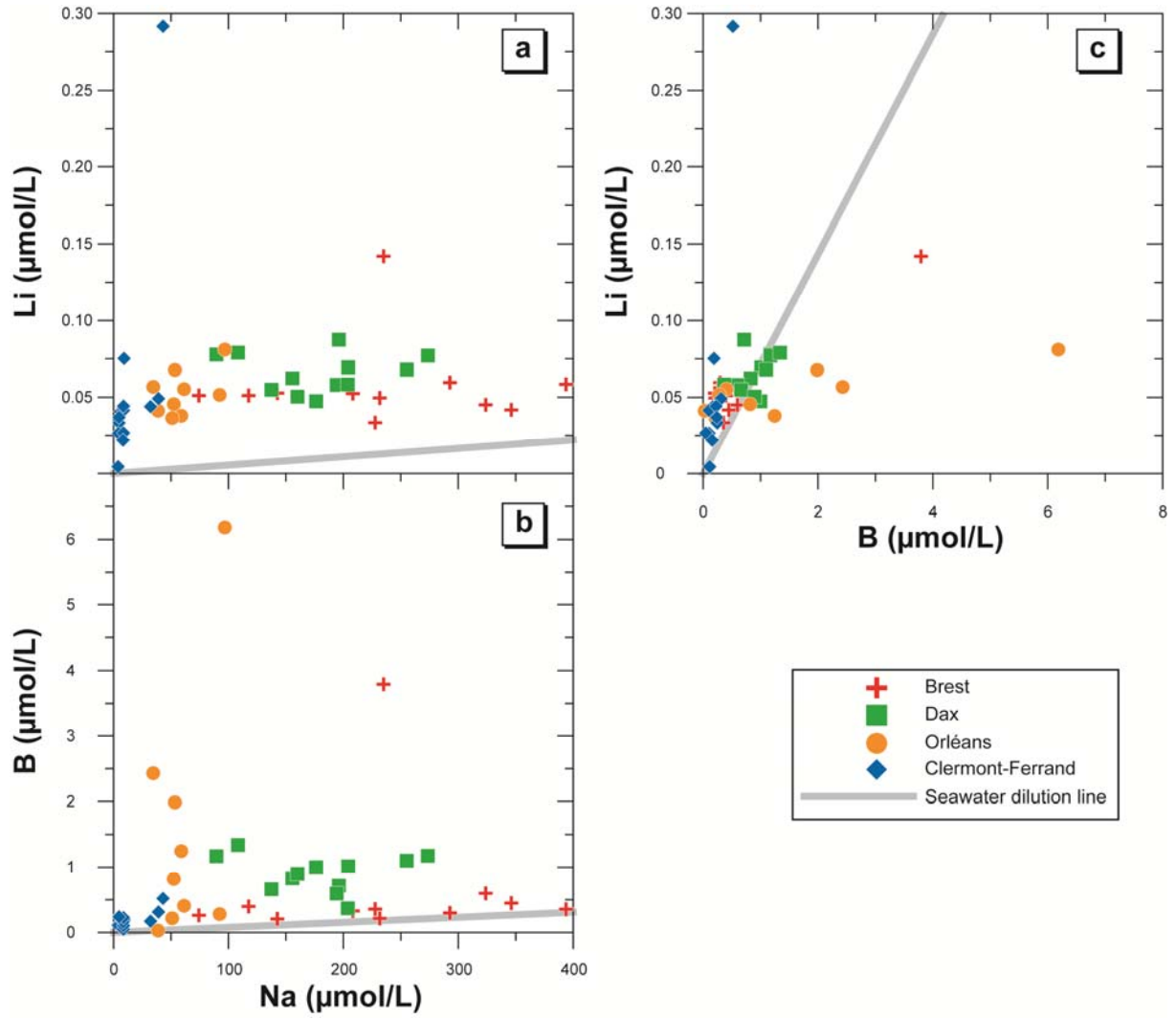
Figure 4



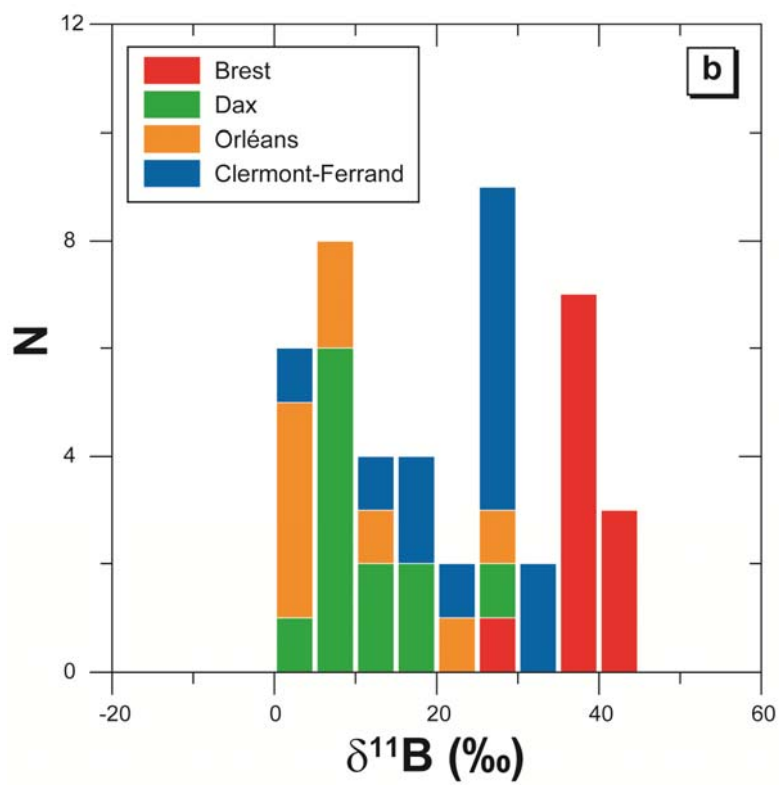
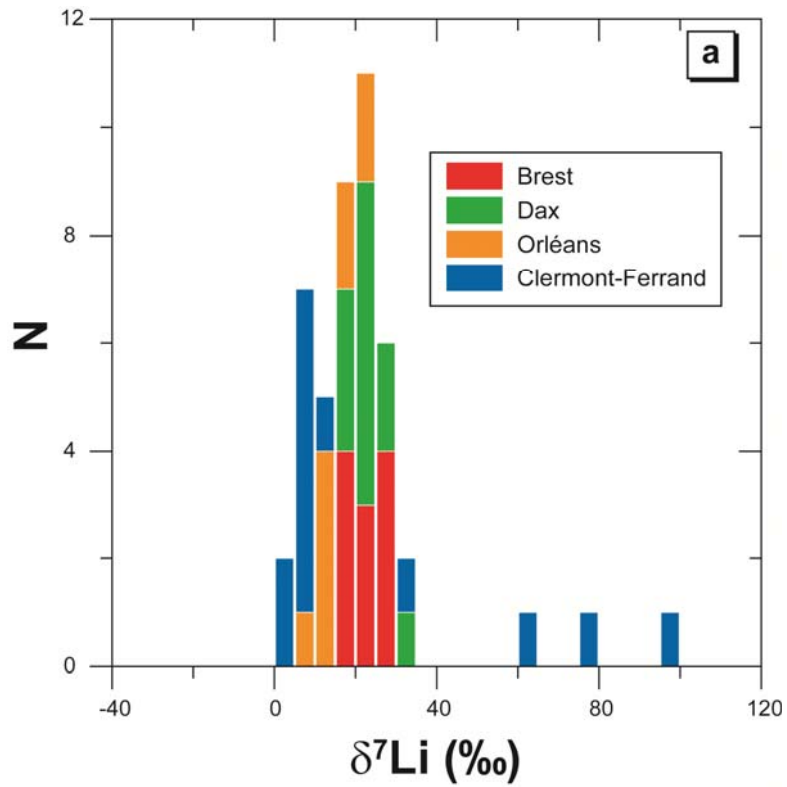
976

977
 978
 979
 980
 981
 982
 983
 984
 985
 986

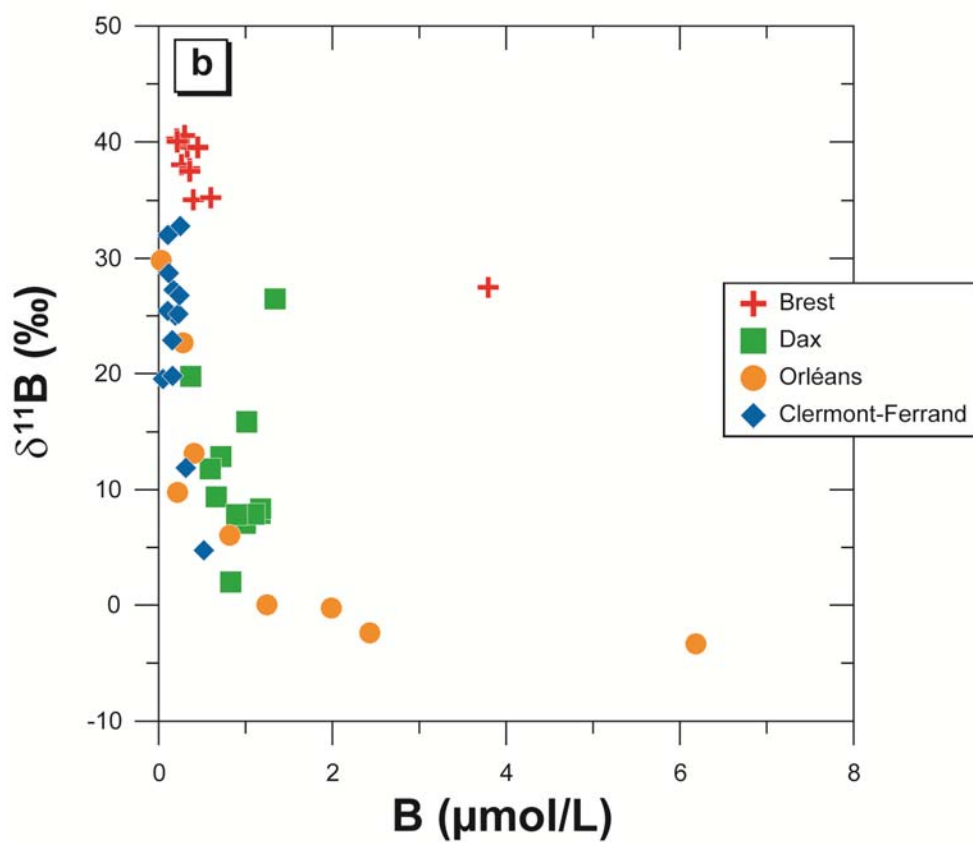
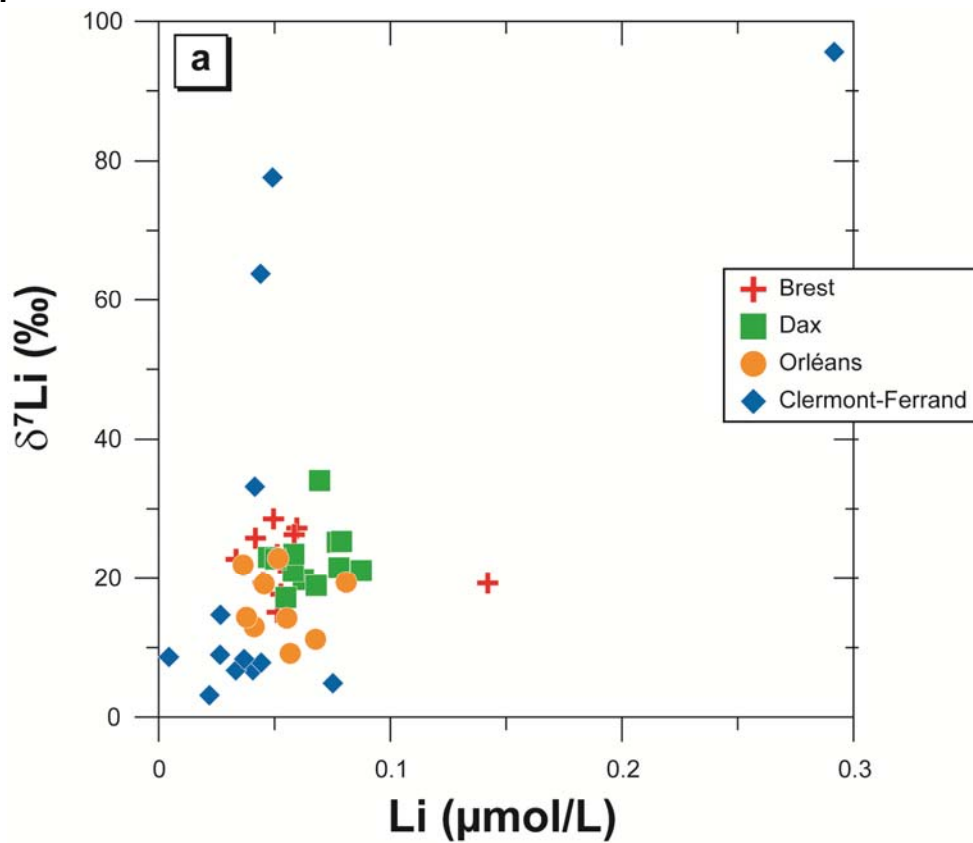
Figure 5



987



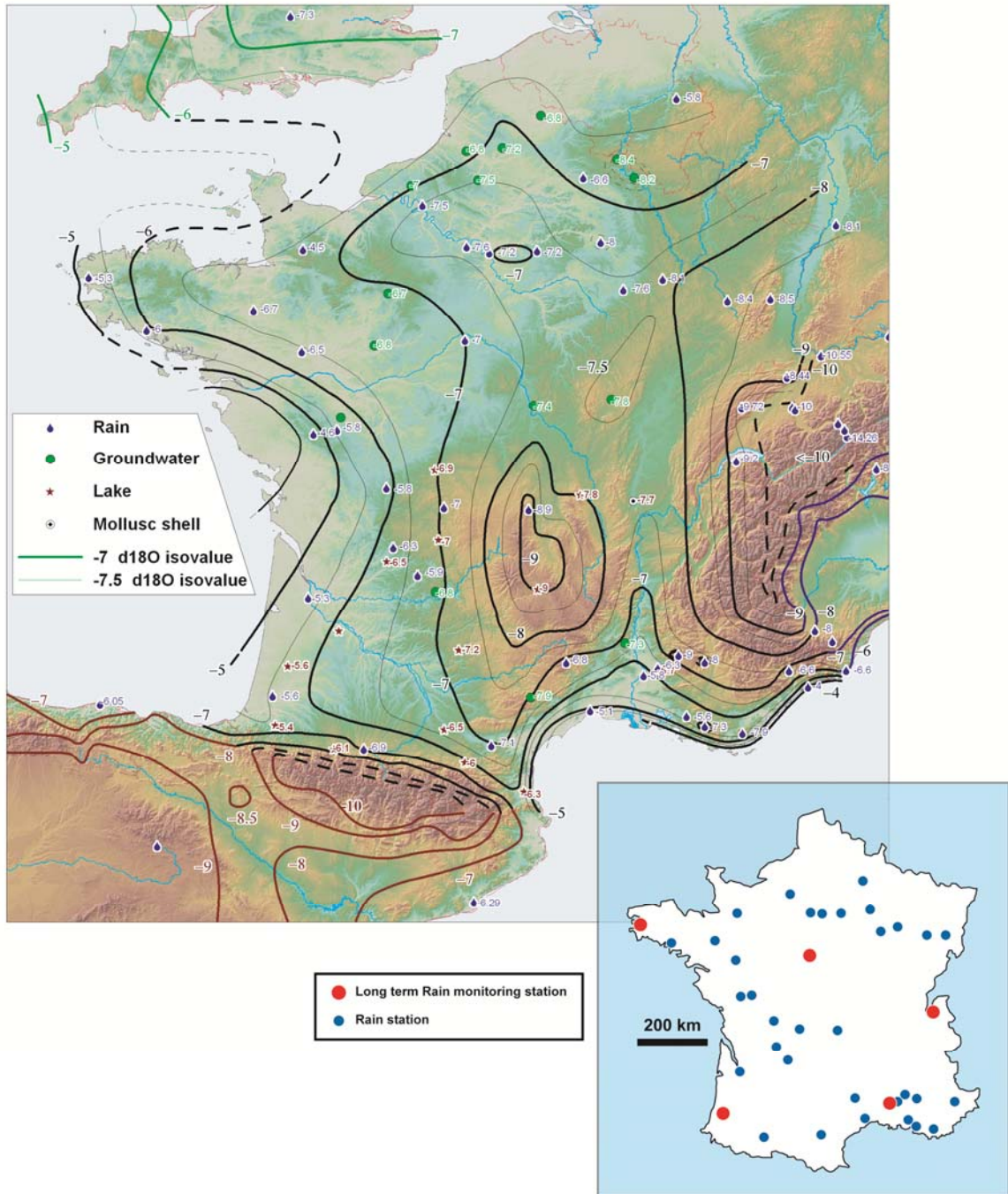
990 **Figure 7**



991

992
993

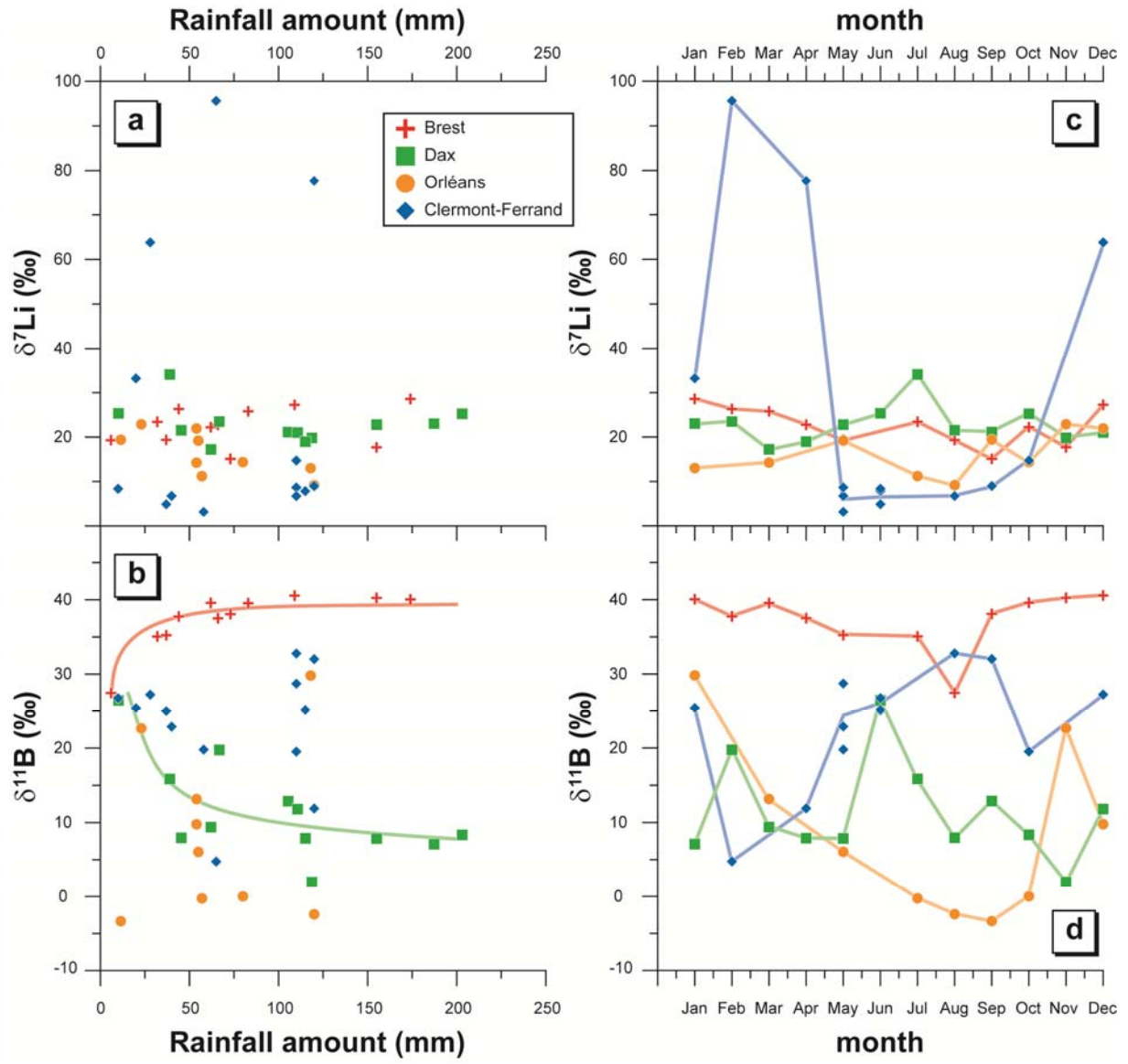
Figure 8



994

995
996
997
998
999
1000
1001
1002
1003

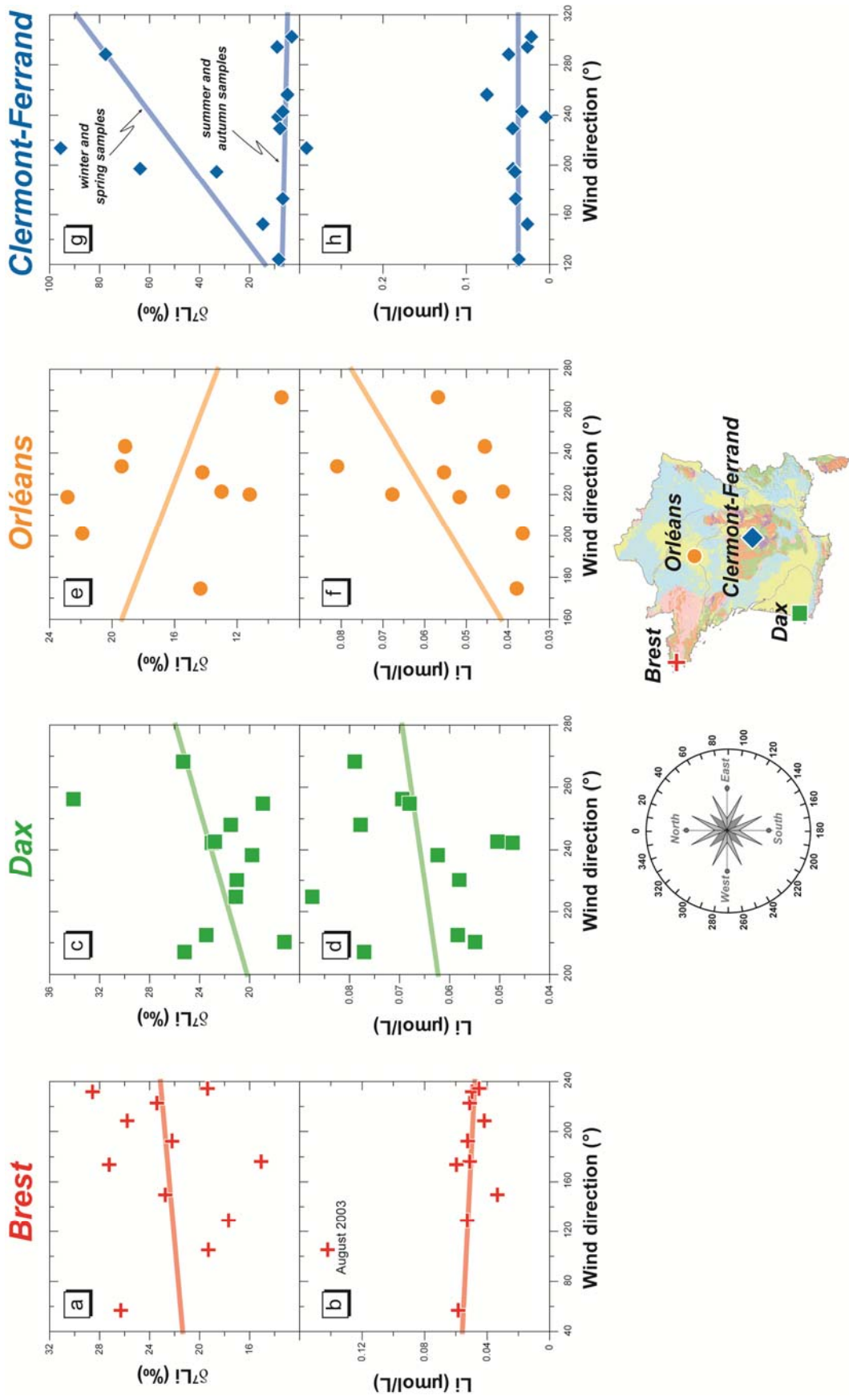
Figure 9



1004
1005

1006
1007

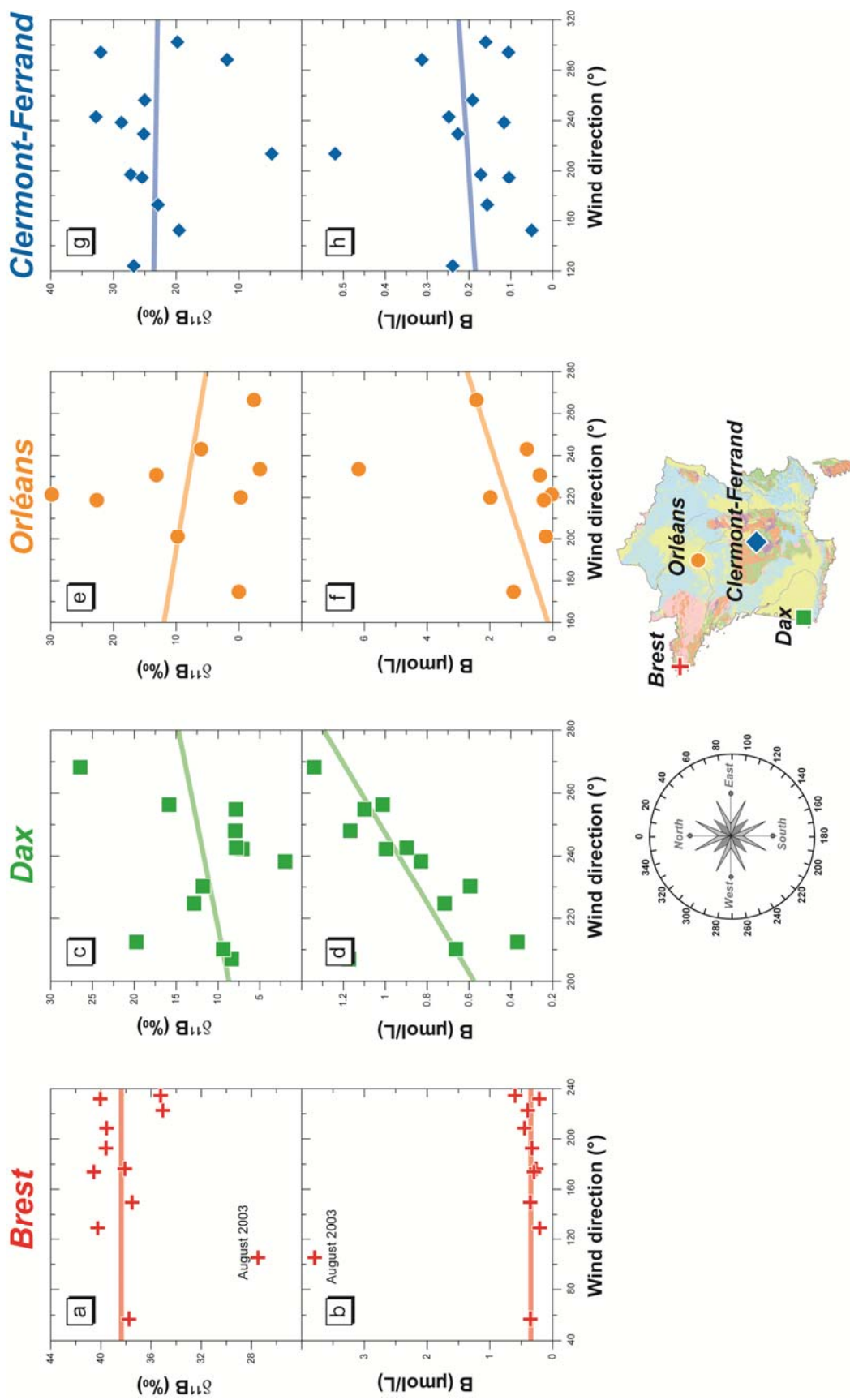
Figure 10



1008
1009

1010
1011

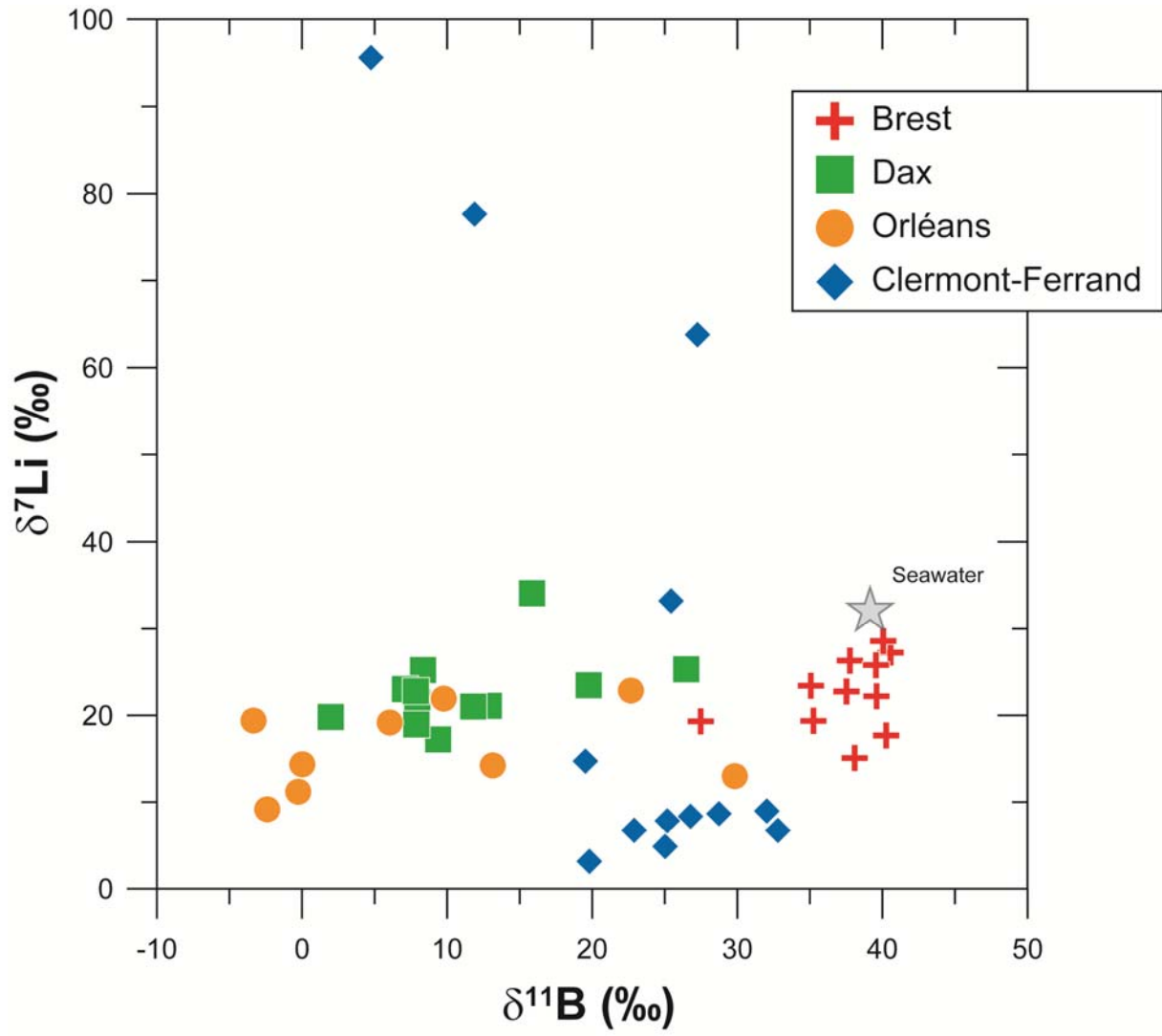
Figure 11



1012

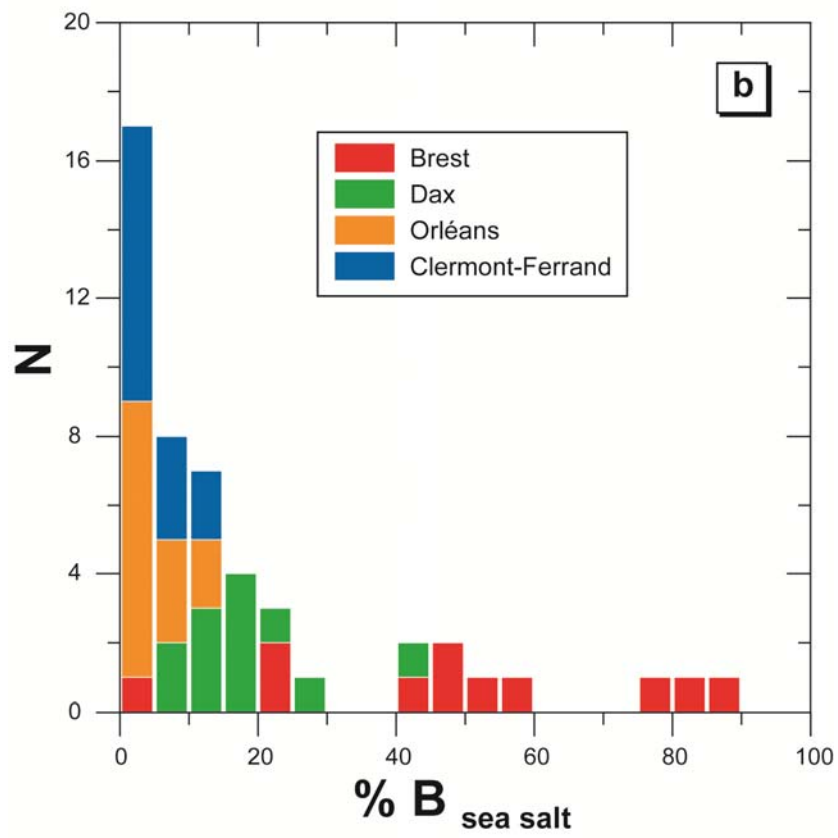
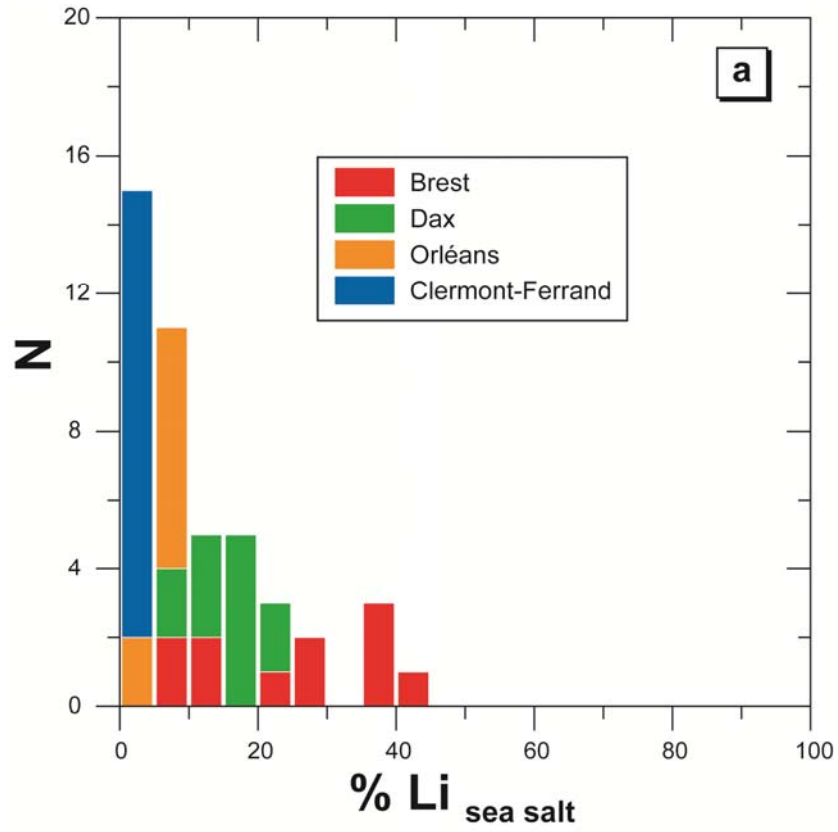
1013
1014
1015
1016
1017
1018
1019
1020
1021

Figure 12



1022

1023 **Figure 13**

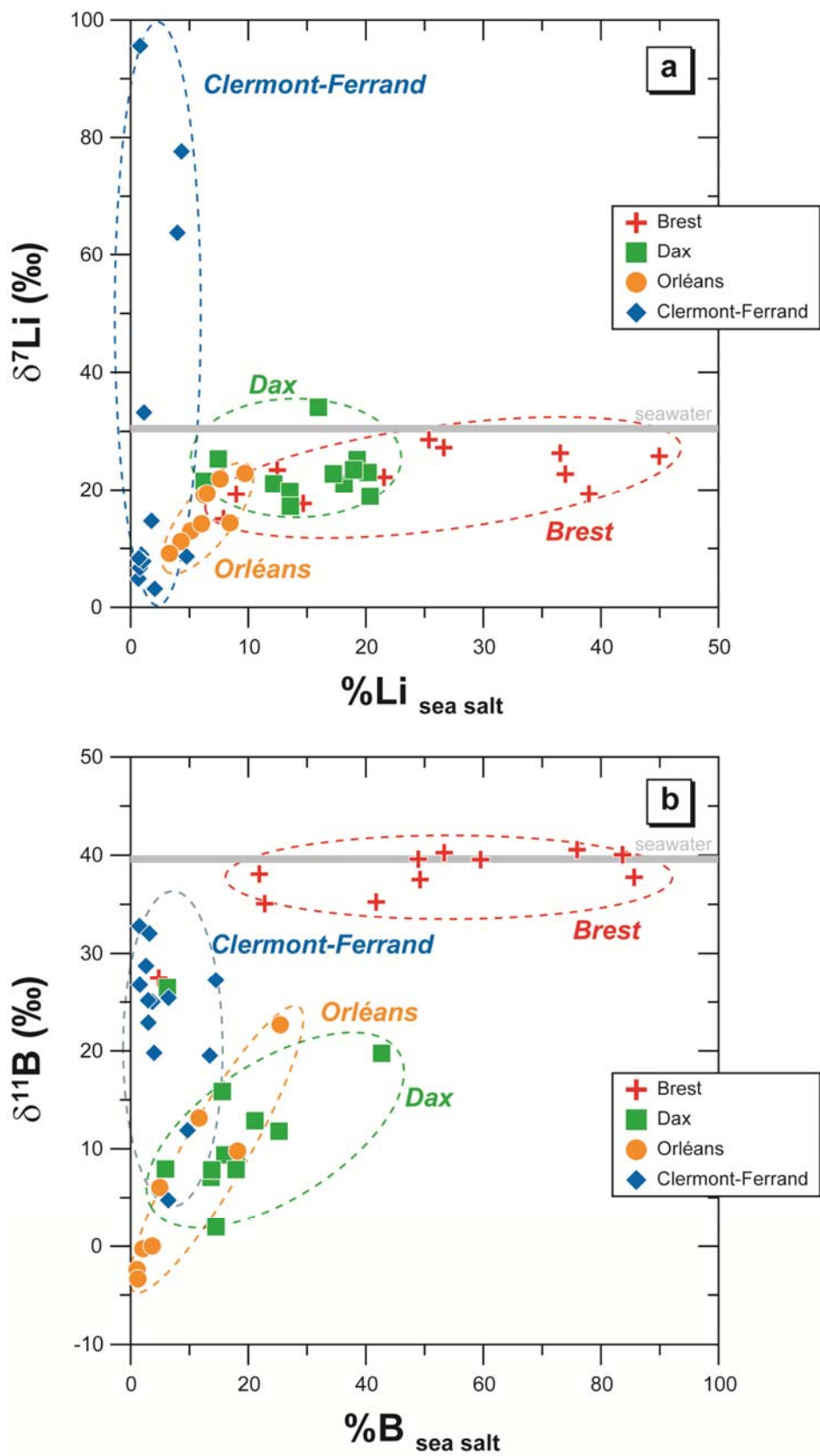


hal-00553187, version 1 - 6 Jan 2011

1024
1025

1026
1027

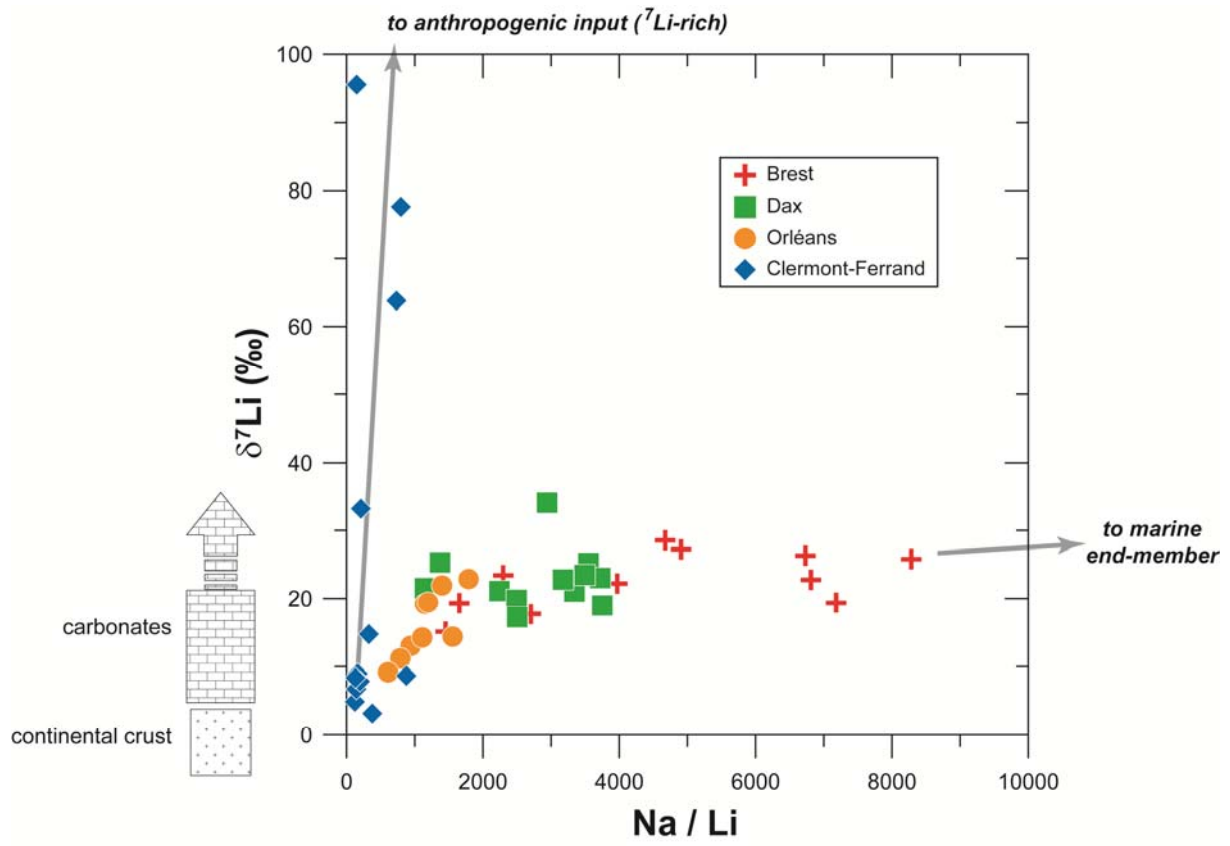
Figure 14



1028

1029
1030
1031
1032
1033
1034
1035
1036
1037

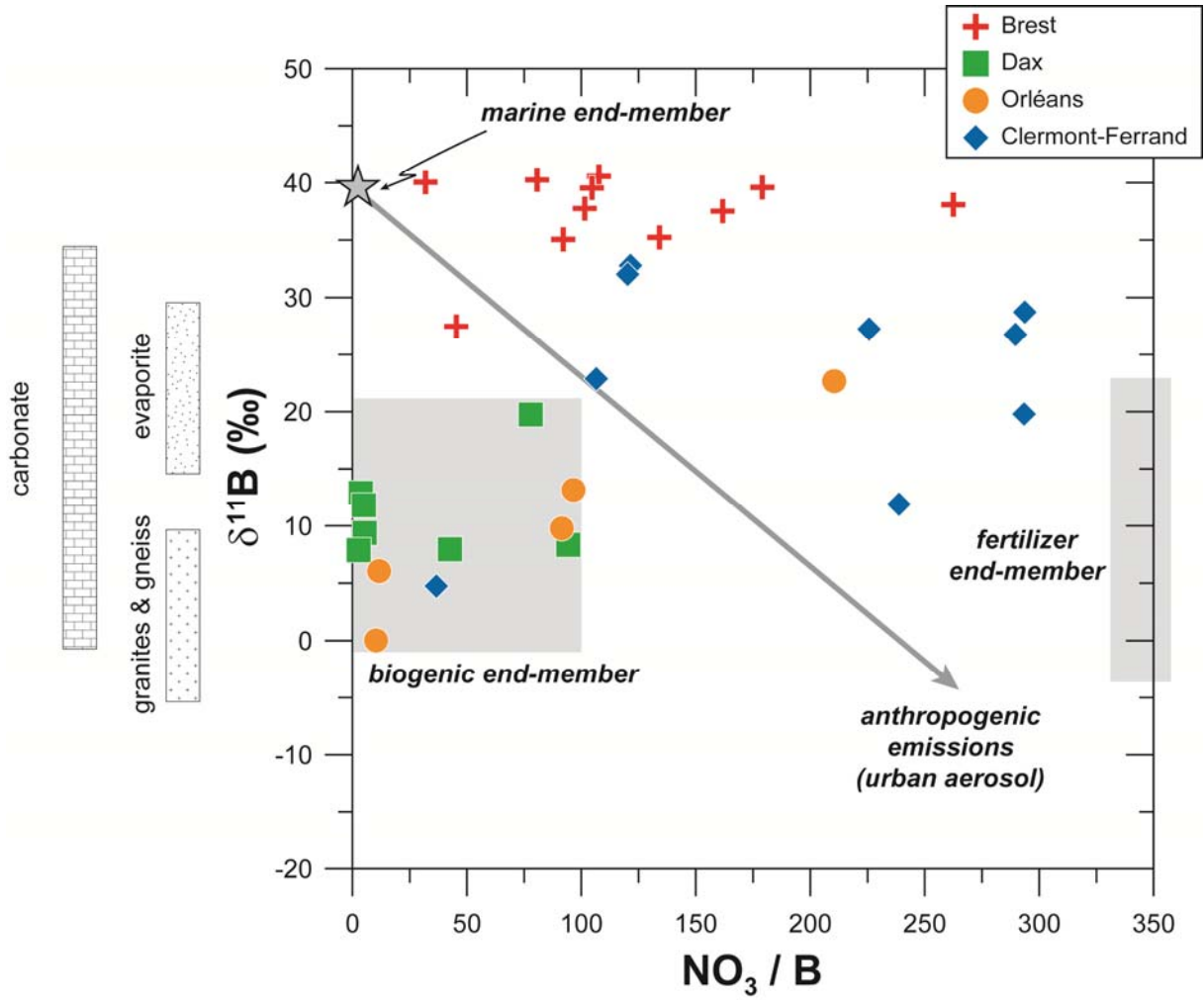
Figure 15



1038

1039
1040
1041
1042
1043
1044
1045
1046
1047

Figure 16



1048